

Cardiopulmonary Resuscitation-Associated Lung Edema (CRALE) - A Translational Study

Aurora Magliocca,^{1,2} Emanuele Rezoagli,² Davide Zani,³ Martina Manfredi,³ Daria De Giorgio,¹ Davide Olivari,¹ Francesca Fumagalli,¹ Thomas Langer,² Leonello Avalli,⁴ Giacomo Grasselli,^{5,6} Roberto Latini,¹ Antonio Pesenti,^{5,6} Giacomo Bellani,^{2,4} Giuseppe Ristagno^{5,6}

¹Department of Cardiovascular Medicine, Istituto di Ricerche Farmacologiche Mario Negri IRCCS, Via G. La Masa 19, 20156 Milan, Italy.

²Department of Medicine and Surgery, University of Milan-Bicocca, Via Cadore 48, 20900, Monza (MB), Italy

³DIMEVET, University of Milan, Lodi, Italy

⁴ Department of Emergency and Intensive Care, San Gerardo Hospital, Monza, Italy

⁵Department of Medical Physiopathology and Transplants, University of Milan, Via Della Commenda 16, 20122, Milano (MI), Italy

⁶Department of Anesthesia, Critical Care and Emergency, Fondazione IRCCS Ca' Granda - Ospedale Maggiore Policlinico, Via Francesco Sforza 35, 20122, Milan (MI), Italy

This article has an online data Supplement, which is accessible for this issue's table of content online at www.atsjournal.org.

Corresponding Author:

Giacomo Bellani, MD, PhD

Department of Medicine and Surgery, University of Milan-Bicocca,

Via Cadore 48, 20900, Monza (MB), Italy

Email: giacomo.bellani1@unimib.it

Phone: +39 039 233 3293

Authors' contributions:

A.M. conceived the study, performed animal experiments, collected, interpreted and analyzed experimental and clinical data, data, analyzed chest CT scan images, searched literature, and wrote the manuscript; E.R. collected clinical data, interpreted and analyzed experimental and clinical data, searched literature, and wrote the manuscript; D.Z. and M.M. performed CT scans in the animal model and analyzed chest CT scan images; D.D.G and D.O. performed animal experiments; F.F. interpreted data and revised the manuscript; T.L. provided clinical data and revised the manuscript; L.A. provided clinical data and revised the manuscript; G.G. provided clinical data and revised the manuscript; R.L. and A.P. interpreted data and revised the manuscript; G.B. supervised the study project, provided clinical data and is the coordinator of the multicenter clinical study, interpreted experimental and clinical data and wrote the manuscript; G.R. conceived the study, performed animal experiments, collected and interpreted animal data, and revised the manuscript.

All authors gave final approval of the version to be published and agreed to be accountable for all aspects of the work in ensuring that questions related to the accuracy and integrity of any part of the work are appropriately investigated and resolved.

Conflict of interest statement:

The authors declare no conflict of interest.

Sources of support:

This study was funded by Institutional funds, and in part by linea 2 University of Milan to GR.

Running head: Cardiopulmonary Resuscitation-Associated Lung Edema

Descriptor number:

4.03 Cardiopulmonary Interactions/CV Performance

8.14 Gas Exchange

9.32 Pulmonary Edema

8.15 Imaging: Animal Models

4.02 ALI/ARDS: Diagnosis & Clinical Issues

Total word count: 3532/3500

At a Glance

What is the current scientific knowledge on this subject?

Cardiac arrest is a leading cause of death worldwide with poor outcome.

Lung injury has been reported in the post cardiac arrest period. Imaging studies using Computed Tomography showed that lung injuries may be detectable in up to 79% of patients undergoing Cardiopulmonary Resuscitation. The effect of different Chest Compression (CC) strategies (mechanical versus manual), leading to different pressures application on the respiratory system has not been investigated so far.

What does this study add to the field?

In this translational study we reported that CPR caused lung edema that was more prominent after mechanical CC compared to manual CC in both swine and out-of-hospital cardiac arrest patients. Mechanical CC was characterized by higher intrathoracic pressure swings which led to increased lung weight, reduced oxygenation and respiratory system compliance compared to the manual CC strategy. The consistent evidence of lung alteration associated with CPR from both animals and humans allows for the introduction of the concept of Cardiopulmonary Resuscitation-associated Lung Edema (CRALE).

Abstract

Rationale: Cardiopulmonary Resuscitation is the cornerstone of cardiac arrest (CA) treatment. However, lung injuries associated with it have been reported.

Objectives: To assess 1) the presence and characteristics of lung abnormalities induced by Cardiopulmonary Resuscitation and 2) the role of mechanical and manual chest compression (CC) in its development.

Methods: This translational study included : 1) a porcine model of CA and Cardiopulmonary Resuscitation (n=12), 2) a multicenter cohort of out-of-hospital CA patients undergoing mechanical or manual CC (n=52). Lung Computed Tomography performed after resuscitation was assessed qualitatively and quantitatively along with with respiratory mechanics and gas exchanges.

Measurements and Main Results: The lung weight in the mechanical CC group was higher compared to the manual CC group in the experimental (431 ± 127 vs 273 ± 66 , $p=0.022$) and clinical study (1208 ± 630 vs 837 ± 306 , $p=0.006$). The mechanical CC group showed significantly lower oxygenation ($p=0.043$) and respiratory system compliance (Cpl,rs) ($p<0.001$) compared to the manual CC group in the experimental study. The variation of right atrial pressure was significantly higher in the mechanical compared to the manual CC group (54 ± 11 vs 31 ± 6 mmHg, $p=0.001$) and significantly correlated with lung weight ($r=0.686$, $p=0.026$) and Cpl,rs ($r=-0.634$, $p=0.027$). Incidence of abnormal lung density was higher in patients treated with mechanical compared to manual CC (37% vs 8% , $p=0.018$).

Conclusions: This study demonstrated the presence of Cardiopulmonary Resuscitation Associated Lung Edema (CRALE) in animals and in out-of-hospital CA patients, which is more pronounced after mechanical- as opposed to manual CC and correlates with higher

swings of right atrial pressure during CC.

Abstract word count: 250/250

Key words:

Cardiac arrest; Cardiopulmonary resuscitation; Acute lung injury; Chest compression;

Intrathoracic pressure

Introduction

Cardiac arrest (CA) is a leading cause of death worldwide (1). Despite early initiation of cardiopulmonary resuscitation (CPR) and prompt defibrillation have increased the rate of return of spontaneous circulation (ROSC), CA outcome remains poor. Only 12% of out-of-hospital CA patients survive to hospital discharge, and barely 8% of these survivors regain good neurological recovery (1).

The high mortality rate after successful resuscitation from CA is attributed to the “post-CA syndrome” (2-3); a post-reperfusion state characterized by systemic inflammation leading to multiple organ dysfunction. Recently, a non-negligible incidence of lung injury in the post-CA period has been demonstrated (4-5). Up to 50% CA survivors develop acute respiratory distress syndrome (ARDS) within 48h after hospital admission, and this early ARDS is associated with hospital mortality and poor neurological outcome (4). Indeed, a post-resuscitation lung protective ventilation strategy is suggested, as low tidal volume ventilation may improve neurocognitive outcome after CA. In a study comparing a tidal volume lower or higher than 8 ml kg^{-1} in out-of-hospital CA survivors, it was observed that a lower tidal volume in the first 48 h post-ROSC was associated with a favorable neurological outcome, more ventilator and shock-free days (5).

The different risk factors associated with lung injury after CA include pulmonary ischemia–reperfusion, aspiration of gastric content, pulmonary contusion from chest compression, and systemic inflammation (6-8). Autopsy-based comparison between manual and mechanical chest compression (CC) revealed that lung lesions are present respectively in 4% and 18.6% of patients undergoing manual and mechanical CCs respectively (9). Imaging studies using Computed Tomography (CT) showed that lung injuries may be detectable in up to 79% of patients undergoing CPR (10-11). Despite these observations, a radiological

(qualitative and quantitative CT scan analysis) and functional description of lung abnormalities after CPR is lacking, especially after the introduction of mechanical CC. Furthermore, pressure applied to the respiratory system generated by different CC strategies (mechanical versus manual), has not been investigated so far. Accordingly, the aim of this study was to systematically assess the presence of lung abnormalities associated with cardiopulmonary resuscitation- and to evaluate whether mechanical and manual chest compression (CC) could play a different role in the development of these in a porcine model of CA. We then corroborated our observations in a retrospective multicenter observational cohort study including non-traumatic out-of-hospital CA patients with a lung CT scan at hospital admission.

Methods

This study encompassed two phases. Lung abnormalities were first investigated in a porcine model of CA and prolonged mechanical vs manual CPR and then in a cohort of out-of-hospital CA patients undergoing mechanical or manual CC with a lung CT scan performed after resuscitation.

Experimental study

This is a secondary analysis of a previous study (12). In an ambulance transport, pigs in CA were randomized to 18 min of mechanical or manual CC.

After 2 min of CA, continuous CC was started simultaneously to unsynchronized mechanical ventilation. Manual CC was provided in accordance to 2015 international CPR guidelines (13). Mechanical CC was delivered by the LUCAS® 3.0 chest compression system (Stryker/Jolife AB, Lund, Physio-Control, Sweden), delivering continuous CC (rate: 102 ± 2 per min; depth: 53 ± 2 mm; duty cycle: $50 \pm 5\%$). Every 5 min during CPR, epinephrine (1 mg)

was administered.

Defibrillation was attempted with a biphasic 200-Joule shock. ROSC was defined as the presence of sinus rhythm with a mean arterial pressure of more than 60 mmHg.

Measurements

ECG, hemodynamics, EtCO₂, were continuously recorded. For each minute of CPR the minimum, the maximum and the swing in right atrial pressure were computed. The variation of right atrial pressure (Δ RAP) was reported as surrogate of intrathoracic pressure (ITP). Dynamic compliance of the respiratory system (Cpl,rs) was assessed. Arterial blood gas analyses were obtained. Plasma high-sensitivity cardiac troponin T (hs-cTNT), N-Terminal Pro-Atrial Natriuretic Peptide (NTpro-ANP), receptor for advanced glycation end product (RAGE) and pulmonary surfactant associated protein D (SPD) were measured with ELISA assays.

CT scanning and morphological analysis

All successfully resuscitated animals underwent lung CT scan at the end of resuscitation maneuvers (n=12, mechanical n=6 or manual n=6), performed during breath holding at end-expiration. Two veterinary radiologists, blind to study groups, assessed lung CT scans in order to describe the morphological lung alterations (14).

Clinical study

This was a multicenter observational, retrospective cohort study. The Ethical Committee of each enrolling hospital approved the study (Ethical Committee N° 3070). Informed consent was waived from the Ethical Committee due to the retrospective observational nature of the

investigation and CA patients admitted from 2011 to 2019 in the intensive care units (ICU) of three hospitals were enrolled.

Inclusion criteria were adult out-of-hospital non-traumatic CA who received manual or mechanical CC with a lung CT scan performed within 24h. Exclusion criteria were aspiration pneumonia and/or pulmonary embolism.

Since CT scan was performed as part of the diagnostic work-up of the patients, scans occurred during uninterrupted ventilation, as per clinical practice.

The following clinical data were retrieved from patient electronic medical records: sex, age, weight, CA characteristics, physiological data including gas exchanges and ventilator setting, ICU and hospital length-of-stay and hospital mortality.

Lung CT quantitative analysis

Quantitative analysis of lung CT scans of experimental CAs and out-of-hospital CA patients were performed using manual segmentation in blind and published methods for volume and weight measurements (15-17).

A threshold of 500 HU (17) of mean lung CT was used in order to define average lung density as normal (mean lung CT < 500) or below normal (mean lung CT \geq 500).

Statistical analysis

Continuous and categorical data were expressed as mean \pm standard deviation or frequency (percentage), respectively. Differences among groups were assessed with parametric or non-parametric tests as appropriate. Fisher's exact test was used for categorical data. In the morphological analysis of the CT scan findings, the presence of ground glass attenuation (GGA) and airspace consolidation (AC) were evaluated in each of the six lung lobes of each

animal. In order to adjust the model for the within animal correlation, difference among groups in the proportion of GGA and AC was calculated using an adjusted logistic regression analysis with robust clustering, where GGA and AC were considered as outcome variable, the type of chest compressions as exposure variable, and the pigs were considered as cluster variable. Correlations between continuous data were explored using linear regression analyses. Statistical significance was set at $p\text{-value}<0.05$ (two-tailed).

Please refer to the online data supplement for detailed methods.

Results

Experimental study

Figure 1 shows a representative CT image of pigs receiving mechanical or manual CC; the graph below shows that the mean lung weight was significantly higher when a mechanical CC device was used. Table 1 shows the morphological analysis of animals' lung CTs. The ground glass attenuation was present in both groups, affecting a significantly higher fraction of lobes with diffuse pattern in the mechanical CC compared to the manual CC group (83% vs 25%, $p<0.001$). The airspace consolidations were detected more frequently in the mechanical CC group compared to the manual CC one (72% vs 42%, $p=0.012$). Peribronchovascular thickening, interlobular thickening, air bronchogram, pleural effusion and rib fractures were not significantly different between the two groups. The proportion of animals affected by ground glass attenuation and airspace consolidation stratified by lung lobes is illustrated in Table E1 and Figure 2.

Data regarding the main quantitative CT variables in animals are summarized in Table 2. The lung volume was higher in the mechanical CC group compared to the manual group ($p=0.043$). The lung weight was higher in the mechanical CC group compared to the manual

one ($p=0.022$). The poorly inflated tissue was higher in the mechanical CC group compared to the manual one ($p=0.023$) and accordingly the well-inflated tissue was less represented in the mechanical CC group ($p=0.029$).

The lung density shows a gravitational gradient in both the mechanical and manual CC group. The lung density is higher in the mechanical versus manual CC group at each gravitational level (treatment effect $p=0.018$, Figure 3, panel A). Furthermore, the mechanical CC group shows a higher ventro-dorsal gradient compared to the manual one ($p<0.05$, Figure 3, panel B).

The $\text{PaO}_2/\text{FiO}_2$ was significantly lower in the mechanical CC group compared to the manual group overtime (group-by-time interaction $p=0.043$) (Figure 4A) with return to baseline values 3h after ROSC. The PaCO_2 was higher in the mechanical CC group compared to the manual one (group-by-time interaction $p<0.001$) (Figure 4B). Cpl_{rs} decreased significantly after CPR, with a more severe decline in the mechanical CC group compared to the manual one (group-by-time interaction $p<0.001$) (Figure 4C). Furthermore, the Cpl_{rs} was negatively associated with both total lung weight ($r=-0.723$, $p=0.008$) (Figure E1A) and total lung volume ($r=-0.691$, $p=0.013$) (Figure E1B).

The variation of right atrial pressure (ΔRAP) generated by CCs is represented in Figure 5A. Higher ΔRAP during CC was observed in the mechanical CC group compared to the manual CC group (54 ± 11 vs 31 ± 6 mmHg, $p=0.001$). ΔRAP was positively correlated to the lung weight ($r=0.686$, $p=0.026$) (Figure 5B) and negatively correlated to the Cpl_{rs} ($r=-0.634$, $p=0.027$) (Figure 5C). A representative image of the RAP waveform during CC is reported in Figure E2; differences in ΔRAP between the two groups over 18 min CPR is reported in Figure E3. Hemodynamics and plasmatic levels of biomarkers over time together with lung

histology at 72 hours after ROSC did not show significant changes among groups (Table E2, Figure E4-E5).

Clinical study

During the observation period, 52 patients received a lung CT scan within 24h from CA. Patients' demographic and outcome data are reported in Table 3. CA patients undergoing mechanical CC were significantly younger ($p=0.009$) and with a 2-fold higher low-flow time ($p<0.001$) compared to the group receiving manual CC. Ten out of 16 patients receiving mechanical CC underwent veno-arterial extracorporeal membrane oxygenation (v-a ECMO) while none of the patients in the manual CC group was treated with v-a ECMO ($p<0.001$).

Quantitative analysis of CT scans revealed that mean lung weight was significantly higher in the mechanical CC group compared to manual group ($p=0.006$) (Table 4). The lung volume and the lung gas volume did not differ among the two groups. The amount of not inflated lung tissue was significantly higher in the mechanical CC group compared to the manual one ($p=0.025$), the poorly inflated lung tissue was higher in the mechanical CC group ($p=0.007$) while the well inflated lung tissue was less represented in the mechanical compared to manual group ($p=0.006$).

Table 5 shows the first arterial blood gas analysis and ventilator setting of CA patients at ICU admission and after 24 h. pH, base excess and lactate level were significantly higher in the mechanical CC group compared to the manual one. Mechanical CC treated patients showed a lower $\text{PaO}_2/\text{FiO}_2$ compared to the manual CC group at ICU admission ($p=0.013$) and at 24 h ($p=0.027$). Hemodynamics at ICU admission are represented in table E4.

Exploratory incidence of abnormal lung density in the preclinical and clinical investigation

In the experimental study we observed a higher incidence of abnormal lung density in the

mechanical compared to the manual CC group, despite a non statistical significance (4/6 versus 1/6, 67% versus 17%, $p=0.242$).

In the clinical study, we confirmed a significantly higher proportion of abnormal lung density in the mechanical CC group (6/16 versus 3/36, 37% versus 8%, $p=0.018$). We explored the role of age and low-flow time on abnormal lung density as they differ between mechanical versus manual CC group (Table 3). We observed that mechanical CC (OR 6.6; 95%CI, 1.39–31.28; $p=0.017$) and a trend to a prolonged low flow time (OR 4.42; 95%CI, 0.82–23.79; $p=0.083$) were associated to a higher risk of abnormal lung density (Table E4A). These findings were confirmed using mean lung CT as outcome variable (Table E4B).

We further investigated in 4 independent linear regression models (Model A-D) the association between low-flow time and type of CC with the mean lung CT (Table E5). To include interdependency among the 4 groups of patients, we performed a non-parametric analysis. Patients undergoing mechanical CC with a prolonged CPR showed a significantly higher mean lung density than patients undergoing manual CC with a shorter low-flow time ($p<0.01$), and a trend to a higher mean lung density compared to patients undergoing manual CC with a prolonged low-flow time ($p=0.080$) (Figure 6).

Discussion

In this translational study we provide a comprehensive description of lung abnormalities following cardiopulmonary resuscitation, with similar techniques, in both pigs and humans. The consistent clinical and experimental findings allow us to introduce the concept of “Cardiopulmonary-Resuscitation Associated Lung Edema” (CRALE), as detailed in the following paragraphs. In a preclinical model of CA in pigs, CPR caused lung abnormalities that were more prominent after mechanical CC compared to manual CC. Mechanical CC led to increased lung weight, reduced lung aeration, and reduced oxygenation and compliance

compared to the manual CC strategy. The intensity of intrathoracic pressure swings generated by mechanical CC (assessed by variation in right atrial pressure) was associated with higher lung weight and reduced Cpl,rs. The clinical study confirmed that presence of increased lung density was more frequent after mechanical versus manual CC (37% versus 8%, respectively) in keeping with what observed in the animals (67% versus 17%, respectively). Moreover, the lung weight and the amount of not aerated lung tissue were markedly increased when a mechanical CC strategy was used. This was accompanied by a lower PaO₂/FiO₂, even with a higher PEEP level.

Comparison with existing literature

In CA patients lung damage related to CPR has been described since the 80's (18). Lung injuries detected by CT scan seem frequent complication in CA patients who undergo CPR (11-12). An autopsy-based study demonstrated that mechanical CC leads more often to lung lesions compared to manual CC (10). However, these findings are not unanimously reported (19-22). Moreover, the only randomized non-inferiority safety study comparing mechanical or manual CC, revealed that LUCAS did not cause significantly more serious or life-threatening visceral damage than manual CC (23). Indeed, also in this study mechanical CC did not cause lifethreatening injuries in both animals and humans.

Liu and colleagues described the radiological finding of ground-glass attenuation in pigs 6h after manual resuscitation from either 5 or 10 min of CA (7). Moreover, the authors described the presence of histopathological changes resembled as alveolar flooding, inflammatory cells (i.e. neutrophils), and alveolar barrier disruption suggested by the presence of erythrocytes in the alveolar spaces proportional with the duration of CA (7,8). These experimental studies, however, did not address the effect of mechanical or manual CC.

Characterization of CRALE

In our model, 18 min of CPR led to increased airspace consolidation and ground-glass attenuation in pigs treated with mechanical CC compared to the manual CC group. Further quantitative CT scan analyses were performed after the qualitative ones: these showed that the aeration loss was accompanied by increased lung weight and gravitational gradient, suggesting the presence of lung edema as opposed to sole atelectasis.

In line with the morphological and quantitative lung alterations, gas exchange and respiratory mechanics were impaired during CPR and early after ROSC especially in the mechanical CC treated animals. The compliance of the respiratory system has been reported to decrease after CC, regardless of the technique used (24-26). The aetiology of changes in lung compliance is multifactorial. In our experimental model of CA, mechanical CC treated pigs showed a greater reduction in Cpl,rs 10 min after ROSC together with a higher lung weight and lung volume compared to the manual CC group. These observations suggest an increase in the total amount of fluid in the lung. In addition, a lower PaO₂/FiO₂ was observed in the mechanical CC group compared to the manual one during CPR, at ROSC and up to one hour later, to then recover in the subsequent two hours of observation.

The findings in the cohort of out-of-hospital CA patients were consistent with the animal results. A higher lung weight and amount of not inflated and poorly inflated lung tissue was detected in the mechanical CC group by the quantitative lung CT scan.

Etiology of CRALE

Several possible mechanisms might explain the genesis of CRALE and the greater severity of lung abnormalities in mechanical CC treated animals.

At first, a reduction in lung volume occurs during CC, indeed lung volume during CC

is between Functional Residual Capacity (FRC) and residual volume (27), possibly causing alveolar decrecruitment, atelectrauma and hence aeration and compliance loss.

However, the fundamental role of transmural vascular pressures generated by mechanical CC, in contrast to manual CC, must be taken into account (28-30). In fact Δ RAP during CPR was positively correlated with lung weight and negatively correlated with compliance. This association could also explain the difference among the study groups in lung weight, which is majorly exposed to high pressure swings and negative pressures during the CCs using a mechanical device for CPR. The better hemodynamics generated by the piston-based device might reflect also on the pulmonary blood flow, leading to vascular congestion, as shown in a different setting by Katira et al (31). Pulmonary edema in patients generated by negative intrathoracic pressure has been previously reported (32-34). When the interstitial pressures become negative the hydrostatic pressure gradient increases leading to transcapillary flow with alveolar flooding (35) and inflammation (36). Interestingly, Scharf et al demonstrated that negative-pressure pulmonary edema is more pronounced in patients with myocardial dysfunction (37). The transient nature of CRALE and the lack of difference in biochemical or histological markers of epithelial lung injury favours the hypothesis of an hydrostatic nature of the edema as opposed to increased permeability.

Recently, the concept of patient-self inflicted lung injury has highlighted the possible harmful role of the spontaneous patient effort on the development of lung injury. In the presence of acute respiratory failure, the patient's effort leads to extremely low intrathoracic pressure to correct impaired gas exchanges. Although in a different clinical scenario, we believe that CRALE and P-SILI may share the pathophysiological pathway of the negative intrathoracic pressure (38).

Given that the exact mechanisms are still to be identified and that potential

confounders exist (e.g. ischemia/reperfusion (39) and hyperoxia (40) inducing lung injury and atelectasis (41)) it appears more appropriate to consider the edema “associated to-“ as opposed to “induced by-“ CPR .

Strengths and limitations

The experimental study was performed in a scenario simulating a real clinical challenge such as the management of CPR after CA during ambulance transportation, increasing the translation to humans of the experimental findings. Another point of strength is represented by the novelty, since to our knowledge this is the first report describing a comprehensive assessment of lung CT scan with qualitative and quantitative analyses after experimental and clinical CPR.

Several limitations must also be acknowledged. Firstly, it represents a secondary analysis of a randomized preclinical study aimed to compare the hemodynamic effect of mechanical and manual CC strategy, where the pleural pressure was not directly measured; however, CT scan were prospectively obtained with the aim of assess lung aeration and weight. Moreover, biological assessment of lung edema fluid was not available, in order to assess alveolar permeability and inflammation. Secondly, only one ventilation strategy was tested. Whether the role of unsynchronized ventilation is prevalent over CC itself in causing lung injury cannot be excluded and need further studies. Future work is necessary to identify the optimal ventilation strategy and PEEP setting during mechanical CC. Thirdly, we cannot also exclude that the ventilator used accounted for the generation of a closed circuit with the animals airway, similarly to the impedance threshold device (41), ultimately decreasing ITP during CC release and the subsequent lung edema.

The main limitation of the clinical study is the retrospective observational design, which accounted for a great heterogeneity of the out-of-hospital CA population studied.

Patients undergoing mechanical CC were subjected to a significantly longer CPR time and showed a significantly higher proportion of extracorporeal life support. Based on local clinical protocols, mechanical CC is used mainly in CA patients candidate for extracorporeal life support, which is applied in the instance of refractory CA after an interval of at least 15 min of CPR. The presence of both factors was associated with CRALE, but the contribution of each factor has yet to be elucidated.

Moreover, in these patient data on how ventilation during CC was provided are missing. Heterogeneous clinical practice has been reported in ventilator setting and monitoring during CPR, with significant divergence from international recommendations (42). The importance of mechanical ventilation during CPR is suggested to play a key role on outcomes after out-of-hospital CA (43).

Another limitation of the clinical study is that the majority of patients undergoing mechanical CC were candidate for venous-arterial (V-A) ECMO. Lung CT scan was performed when V-A ECMO was already placed. V-A ECMO significantly reduces pulmonary perfusion of the lung with a relative increase of the ventilation perfusion ratio and the potential risk of alveolar alkalosis which could decrease the alveolar fluid reabsorption (44).

Conclusion

In conclusion, our observations highlight the presence of lung abnormalities, likely representing a Cardiopulmonary-Associated Lung Edema (CRALE) which were more pronounced after mechanical versus manual CC, with a derangement in mechanical properties and gas exchange. These alterations are transient and appear related with the intensity of intratoracic pressure swings during CC. Further research should be focused on

the identification of the optimal ventilation strategy in order to prevent or reduce the occurrence of CRALE.

Acknowledgments

The authors want to thank Fabiana Madotto (University of Milan-Bicocca, Monza, Italy) for statistical support; Vanessa Zambelli, Silvia Villa, Valentina Ciceri (University of Milan-Bicocca, Monza, Italy), Carlo Perego (Istituto di Ricerche Farmacologiche Mario Negri IRCCS, Milan, Italy), Alberto Cucino, Giovanni Babini (University of Milan, Milan, Italy) for their valuable support.

Figure legends

Figure 1. Representative CT images of cranial (A) and caudal (B) lung lobes in the mechanical CC (right panels) and in the manual CC (left panels) treated pigs. In the bottom graph (C), differences in the lung weight estimated by CT scan analysis among the experimental groups. L=left lung side.

Figure 2. Morphological distribution of the lung abnormalities stratified by lung lobes and reported as proportion of animals with ground glass attenuation (GGA) and airspace consolidation (AC). In A, lung lobe anatomy in pigs. In B and C, GGA in manual and mechanical CC group, respectively. In D and E, AC in manual and mechanical CC group, respectively.

Figure 3. Differences of lung tissue density among groups at each gravitational level expressed as thirds of the lung sterno-costal height from the ventral to the dorsal lung areas (A). Difference in the gradient of lung density from the ventral to the dorsal regions among groups (B). The gradient of lung density was calculated as $(\text{Ventral HU} - \text{Dorsal HU}) / (\text{ventral HU}) * 100$. *, $p < 0.05$; **, $p < 0.01$.

Figure 4. Differences of $\text{PaO}_2/\text{FiO}_2$ (A) and PaCO_2 (B) between the groups at baseline, during CPR and within 3 hours after ROSC. Differences of dynamic respiratory compliance (Cpl_{rs}) between the groups at baseline and at 3 hours after ROSC (C). In A and B data are expressed as whisker plots. In C data are represented as $\text{mean} \pm \text{SD}$. Group-by-time interaction p-value of the repeated measurements two-way ANOVA was reported. In A, at 5 minutes post-ROSC there was a trend in the difference of $\text{PaO}_2/\text{FiO}_2$ between the study groups ($p = 0.068$). * $p < 0.05$, ** $p < 0.01$, and *** $p < 0.001$ versus Manual group.

Figure 5. A) Differences of right atrial pressure variation (Δ RAP) between the two animal groups. Association of Δ RAP with lung weight (B) and dynamic compliance of the respiratory system (C). In A data are expressed as mean \pm SD. Duration of exposure to Δ RAP is the same for both experimental groups. In B and C the continuous line represents the best fit line of the linear regression with the 95% CI represented with dashed lines.

Figure 6. Differences of mean lung CT between 4 groups of out-of-hospital cardiac arrest patients stratified by type of CPR and length of low-flow time. Overall difference among groups was tested using a Kruskal-Wallis test. Post-hoc pairwise comparisons among groups were tested using Mann-Whitney U test. CT, computed tomography; HU, Hounsfield unit; CC, chest compression. **, $p < 0.01$.

References

1. Benjamin EJ, Muntner P, Alonso A, Bittencourt MS, Callaway CW, Carson AP, Chamberlain AM, Chang AR, Cheng S, Das SR, Delling FN, Djousse L, Elkind MSV, Ferguson JF, Fornage M, Jordan LC, Khan SS, Kissela BM, Knutson KL, Kwan TW, Lackland DT, Lewis TT, Lichtman JH, Longenecker CT, Loop MS, Lutsey PL, Martin SS, Matsushita K, Moran AE, Mussolino ME, O'Flaherty M, Pandey A, Perak AM, Rosamond WD, Roth GA, Sampson UKA, Satou GM, Schroeder EB, Shah SH, Spartano NL, Stokes A, Tirschwell DL, Tsao CW, Turakhia MP, VanWagner LB, Wilkins JT, Wong SS, Virani SS; American Heart Association Council on Epidemiology and Prevention Statistics Committee and Stroke Statistics Subcommittee. Heart Disease and Stroke Statistics-2019 Update: A Report From the American Heart Association. *Circulation*. 2019;139(10):e56-e528.
2. Adrie C, Adib-Conquy M, Laurent I, Monchi M, Vinsonneau C, Fitting C, Fraise F, Dinh-Xuan AT, Carli P, Spaulding C, Dhainaut JF, Cavaillon JM. Successful cardiopulmonary resuscitation after cardiac arrest as a "sepsis-like" syndrome. *Circulation*. 2002;106(5):562-8.
3. Neumar RW, Nolan JP, Adrie C, Aibiki M, Berg RA, Böttiger BW, Callaway C, Clark RS, Geocadin RG, Jauch EC, Kern KB, Laurent I, Longstreth WT Jr, Merchant RM, Morley P, Morrison LJ, Nadkarni V, Peberdy MA, Rivers EP, Rodriguez-Nunez A, Sellke FW, Spaulding C, Sunde K, Vanden Hoek T. Post-cardiac arrest syndrome: epidemiology, pathophysiology, treatment, and prognostication. A consensus statement from the International Liaison Committee on Resuscitation (American Heart Association, Australian and New Zealand Council on Resuscitation, European Resuscitation Council, Heart and Stroke Foundation of Canada, InterAmerican Heart

Foundation, Resuscitation Council of Asia, and the Resuscitation Council of Southern Africa); the American Heart Association Emergency Cardiovascular Care Committee; the Council on Cardiovascular Surgery and Anesthesia; the Council on Cardiopulmonary, Perioperative, and Critical Care; the Council on Clinical Cardiology; and the Stroke Council. *Circulation*. 2008;118(23):2452-83.

4. Johnson NJ, Caldwell E, Carlbom DJ, Gaieski DF, Prekker ME, Rea TD, Sayre M, Hough CL. The acute respiratory distress syndrome after out-of-hospital cardiac arrest: Incidence, risk factors, and outcomes. *Resuscitation*. 2019;135:37-44.
5. Beitler JR, Ghafouri TB, Jinadasa SP, Mueller A, Hsu L, Anderson RJ, Joshua J, Tyagi S, Malhotra A, Sell RE, Talmor D. Favorable Neurocognitive Outcome with Low Tidal Volume Ventilation after Cardiac Arrest. *Am J Respir Crit Care Med*. 2017;195(9):1198-1206.
6. Johnson NJ, Carlbom DJ, Gaieski DF. Ventilator Management and Respiratory Care After Cardiac Arrest: Oxygenation, Ventilation, Infection, and Injury. *Chest*. 2018;153(6):1466-1477
7. Liu Z, Liu Q, Wu G, Li H, Wang Y, Chen R, Wen C, Ling Q, Yang Z, Tang W. Quantitative CT assessment of lung injury after successful cardiopulmonary resuscitation in a porcine cardiac arrest model of different downtimes. *Quant Imaging Med Surg*. 2018;8(9):946-956.
8. Yang Z, Zheng H, Lin L, Hou J, Wen C, Wang Y, Ling Q, Jiang L, Tang W, Chen R. Alterations in Respiratory Mechanics and Neural Respiratory Drive After Restoration of Spontaneous Circulation in a Porcine Model Subjected to Different Downtimes of Cardiac Arrest. *J Am Heart Assoc*. 2019;8(19):e012441.

9. Ondruschka B, Baier C, Bayer R, Hammer N, Dreßler J, Bernhard M. Chest compression-associated injuries in cardiac arrest patients treated with manual chest compressions versus automated chest compression devices (LUCAS II) - a forensic autopsy-based comparison. *Forensic Sci Med Pathol*. 2018;14(4):515-525.
10. Cho SH, Kim EY, Choi SJ, Kim YK, Sung YM, Choi HY, Cho J, Yang HJ. Multidetector CT and radiographic findings of lung injuries secondary to cardiopulmonary resuscitation. *Injury*. 2013;44(9):1204-7.
11. Cha KC, Kim YW, Kim HI, Kim OH, Cha YS, Kim H, Lee KH, Hwang SO. Parenchymal lung injuries related to standard cardiopulmonary resuscitation. *Am J Emerg Med*. 2017;35(1):117-121.
12. Magliocca A, Olivari D, De Giorgio D, Zani D, Manfredi M, Boccardo A, Cucino A, Sala G, Babini G, Ruggeri L, Novelli D, Skrifvars MB, Hardig BM, Pravettoni D, Staszewsky L, Latini R, Belloli A, Ristagno G. LUCAS Versus Manual Chest Compression During Ambulance Transport: A Hemodynamic Study in a Porcine Model of Cardiac Arrest. *J Am Heart Assoc*. 2019;8(1):e011189.
13. Perkins GD, Handley AJ, Koster RW, Castrén M, Smyth MA, Olasveengen T, Monsieurs KG, Raffay V, Gräsner JT, Wenzel V, Ristagno G, Soar J. Adult basic life support and automated external defibrillation section Collaborators. European Resuscitation Council Guidelines for Resuscitation 2015: Section 2. Adult basic life support and automated external defibrillation. *Resuscitation*. 2015;95:81-99.
14. Judge EP, Hughes JM, Egan JJ, Maguire M, Molloy EL, O'Dea S. Anatomy and bronchoscopy of the porcine lung. A model for translational respiratory medicine. *Am J Respir Cell Mol Biol*. 2014 Sep;51(3):334-43.

15. Chiumello D, Marino A, Brioni M, Cigada I, Menga F, Colombo A, Crimella F, Algieri I, Cressoni M, Carlesso E, Gattinoni L. Lung Recruitment Assessed by Respiratory Mechanics and Computed Tomography in Patients with Acute Respiratory Distress Syndrome. What Is the Relationship? *Am J Respir Crit Care Med* 2016;193:1254–1263.
16. Reske AW, Reske AP, Gast HA, Seiwerts M, Beda A, Gottschaldt U, Josten C, Schreiter D, Heller N, Wrigge H, Amato MB. Extrapolation from ten sections can make CT-based quantification of lung aeration more practicable. *Intensive Care Med*. 2010;36(11):1836-44.
17. Gattinoni L, Pesenti A, Avalli L, Rossi F, Bombino M. Pressure-volume curve of total respiratory system in acute respiratory failure. Computed tomographic scan study. *Am Rev Respir Dis*. 1987;136:730–736.
18. Hillman K, Albin M. Pulmonary barotrauma during cardiopulmonary resuscitation. *Crit Care Med*. 1986;14(7):606-9.31.
19. Smekal D, Lindgren E, Sanderl H, Johansson J, Rubertsson S. CPR-related injuries after manual or mechanical chest compressions with the LUCASTM device: a multicenter study of victims after unsuccessful resuscitation. *Resuscitation*. 2014;85:1708–12.
20. Smekal D, Johansson J, Huzevka T, Rubertsson S. No difference in autopsy detected injuries in cardiac arrest patients treated with manual chest compressions compared with mechanical compressions with the LUCAS device--a pilot study. *Resuscitation*. 2009;80(10):1104-7.
21. Pinto DC, Haden-Pinneri K, Love JC. Manual and automated cardiopulmonary

- resuscitation (CPR): a comparison of associated injury patterns. *J Forensic Sci.* 2013;58:904–909.
22. Lardi C, Egger C, Larribau R, Niquille M, Mangin P, Fracasso T. Traumatic injuries after mechanical cardiopulmonary resuscitation (LUCAS2): a forensic autopsy study. *Int J Legal Med.* 2015;129(5):1035-42.
23. Koster RW, Beenen LF, van der Boom EB, Spijkerboer AM, Tepaske R, van der Wal AC, Beesems SG, Tijssen JG. Safety of mechanical chest compression devices AutoPulse and LUCAS in cardiac arrest: a randomized clinical trial for non-inferiority. *Eur Heart J.* 2017;38(40):3006-3013.
24. Ornato JP, Bryson BL, Donovan PJ, Farquharson RR, Jaeger C. Measurement of ventilation during cardiopulmonary resuscitation. *Crit Care Med.* 1983;11:79–82.
25. Wenzel V, Idris AH, Banner MJ, Kubilis PS, Band R, Williams JL Jr, Lindner KH, Davis KJ, Johannigman JA, Johnson RCJ, Branson RD. Lung compliance following cardiac arrest. *Acad Emerg Med* 1995;2:874–8.
26. Wenzel V, Idris AH, Banner MJ, Kubilis PS, Band R, Williams JL Jr, Lindner KH. Respiratory system compliance decreases after cardiopulmonary resuscitation and stomach inflation: impact of large and small tidal volumes on calculated peak airway pressure. *Resuscitation.* 1998;38(2):113-8.
27. Idris AH, Banner MJ, Wenzel V, Fuerst RS, Becker LB, Melker RJ. Ventilation caused by external chest compression is unable to sustain effective gas exchange during CPR: a comparison with mechanical ventilation. *Resuscitation* 1994;28:143–150.

28. Magder S, Guerard B. Heart-lung Interactions and Pulmonary Buffering: Lessons From a Computational Modeling Study. *Respir Physiol Neurobiol.* 2012;182(2-3):60-70.
29. Broccard AF, Hotchkiss JR, Kuwayama N, Olson DA, Jamal S, Wangenstein DO, Marini JJ. Consequences of vascular flow on lung injury induced by mechanical ventilation. *Am J Respir Crit Care Med.* 1998 Jun;157:1935-42.
30. Katira BH, Giesinger RE, Engelberts D, Zabini D, Kornecki A, Otulakowski G, Yoshida T, Kuebler WM, McNamara PJ, Connelly KA, Kavanagh BP. Adverse Heart-Lung Interactions in Ventilator-induced Lung Injury. *Am J Respir Crit Care Med.* 2017;196(11):1411-1421.
31. Katira BH, Engelberts D, Otulakowski G, Giesinger RE, Yoshida T, Post M, Kuebler WM, Connelly KA, Kavanagh BP. Abrupt Deflation after Sustained Inflation Causes Lung Injury. *Am J Respir Crit Care Med.* 2018;198:1165-1176.
32. Capitanio MA, Kirkpatrick JA. Obstructions of the upper airway in children as reflected on the chest radiograph. *Radiology.* 1973;107(1): 159-161.
33. Oswald CE, Gates GA, Homstrom MG. Pulmonary edema as a complication of acute airway obstruction. *JAMA.* 1977;238(17): 1833-1835.
34. Bhattacharya M, Kallet RH, Ware LB, Matthay MA. Negative-Pressure Pulmonary Edema. *Chest* 2016;150(4):927-933.
35. Loyd JE, Nolop KB, Parker RE, Roselli RJ, Brigham KL. Effects of inspiratory resistance loading on lung fluid balance in awake sheep. *J Appl Physiol.* 1986;60:198-

203.

36. Toumpanakis D, Kastis GA, Zacharatos P, Sigala I, Michailidou T, Kouvela M, Glynos C, Divangahi M, Roussos C, Theocharis SE, Vassilakopoulos T. Inspiratory resistive breathing induces acute lung injury. *Am J Respir Crit Care Med*. 2010;182:1129-36
37. Scharf SM, Woods BO, Brown R, Parisi A, Miller MM, Tow DE. Effects of the Mueller maneuver on global and regional left ventricular function in angina pectoris with or without previous myocardial infarction. *Am J Cardiol*. 1987;59(15):1305-1309.
38. Brochard L, Slutsky A, Pesenti. Mechanical Ventilation to Minimize Progression of Lung Injury in Acute Respiratory Failure. *Am J Respir Crit Care Med*. 2017;195(4):438-442.
39. De Perrot M, Liu M, Waddell TK, Keshavjee S. Ischemia–Reperfusion–induced Lung Injury. *Am J Respir Crit Care Med*. 2003 Feb 15;167(4):490-511.
40. Markstaller K, Rudolph A, Karmrodt J, Gervais HW, Goetz R, Becher A, David M, Kempster OS, Kauczor HU, Dick WF, Eberle B. Effect of chest compressions only during experimental basic life support on alveolar collapse and recruitment. *Resuscitation*. 2008;79:125-32.
41. Budinger GRS, Mutlu GM, Urich D, Soberanes S, Buccellato LJ, Hawkins K, Chiarella SE, Radigan KA, Eisenbart J, Agrawal H, Berkelhamer S, Hekimi S, Zhang J, Perlman H, Shumacker PT, Jain M, Chandel NS. Epithelial cell death is an important contributor to oxidant-mediated acute lung injury. *Am J Respir Crit Care Med* 2011;183:1043–1054.

42. Kwon Y, Debaty G, Puertas L, Metzger A, Rees J, McKnite S, Yannopoulos D, Lurie K. Effect of regulating airway pressure on intrathoracic pressure and vital organ perfusion pressure during cardiopulmonary resuscitation: a non-randomized interventional cross-over study. *Scand J Trauma Resusc Emerg Med.* 2015;23:83.
43. Cordioli RL, Brochard L, Suppan L, Lyazidi A, Templier F, Khoury A, Delisle S, Savary D, Richard JC. How Ventilation Is Delivered During Cardiopulmonary Resuscitation: An International Survey. *Respir Care.* 2018;63(10):1293-1301.
44. Chang MP, Lu Y, Leroux B, Aramendi Ecnarro E, Owens P, Wang HE, Idris AH. Association of ventilation with outcomes from out-of-hospital cardiac arrest. *Resuscitation.* 2019;141:174-181.
45. Myrianthefs PM, Briva A, Lecuona E, Dumasius V, Rutschman DH, Ridge KM, Baltopoulos GJ, Sznajder JJ. Hypocapnic but not metabolic alkalosis impairs alveolar fluid reabsorption. *Am J Respir Crit Care Med.* 2005;171(11):1267-71.

Table 1. Lung morphological CT-scan analysis in the experimental study

	Manual CC (n=6)	Mechanical CC (n=6)	p-value
Ground Glass Attenuation	36 lung lobes	36 lung lobes	
Presence, n (%)	28/36 (78)	34/36 (94)	0.144
• Local, n (%)	19/36 (53)	4/36 (11)	<0.001
• Diffuse, n (%)	9/36 (25)	30/36 (83)	<0.001
Airspace consolidation	36 lung lobes	36 lung lobes	
Presence, n (%)	15/36 (42)	26/36 (72)	0.012
• Local, n (%)	7/36 (19)	11/36 (30)	0.342
• Diffuse, n (%)	8/36 (22)	15/36 (42)	0.147
Peribronchovascular thickening, n (%)	4/6 (67)	4/6 (67)	1.000
Interlobular septal thickening, n (%)	1/6 (17)	5/6 (83)	0.080
Air bronchogram, n (%)	3/6 (50)	6/6 (100)	0.182
Pleural effusion, n (%)			
• Right	0/6 (0)	1/6 (17)	1.000
• Left	0/6 (0)	0/6 (0)	/
• Bilateral	0/6 (0)	0/6 (0)	/
Bone fractures and dislocations, n (%)			
Rib fractures			
• Incomplete	4/6 (67)	5/6 (83)	1.000
• Complete			
- Compound	3/6 (50)	5/6 (83)	0.545
- Dislodged	4/6 (67)	2/6 (33)	0.567
Sterno-costal dislocation	1/6 (17)	1/6 (17)	1.000

Table 2. Lung CT-scan quantitative analysis in the experimental study

	Manual CC (n=6)	Mechanical CC (n=6)	p-value
Lung density, HU	-548±45	-457±74	0.028
Lung volume, mL	601±111	782±157	0.043
Lung gas Volume, mL	327±55	352±65	0.498
Lung weight, g	273±66	431±127	0.022
Not inflated lung tissue, %	2±3	9±9	0.100
Poorly inflated lung tissue, %	32±11	49±11	0.023
Well inflated lung tissue, %	66±13	41±20	0.029

Data expressed as mean±SD.

Table 3. Baseline characteristics and outcomes of out-of-hospital CA patients.

	Manual CC (n=36)	Mechanical CC (n=16)	p-value
Demographic Characteristics			
Age, years (mean±SD)	63±13	52±17	0.009
Gender, M/F, %	22/14 (61/39)	10/6 (63/37)	1.000
Weight, kg	74±18	78±16	0.223
Cardiac Arrest Characteristics			
Bystander-performed CPR, n (%)	22 (61)	12 (75)	0.528
No-flow time, min (mean±SD)	5±4	3±4	0.123
Low-flow time, min (mean±SD)	22±11	55±26	<0.001
First monitored rhythm, n (%)			0.560
• Shockable	17/36 (47)	6/16 (38)	
• Non-shockable	19/36 (53)	10/16 (62)	
Hospital procedures			
ECMO v-a, n (%)	0 (0)	10 (62)	<0.001
IABP, n (%)	0 (0)	1 (6)	0.300
Coronary angiography, n (%)	19 (53)	8 (50)	1.000
Cardiac surgery, n (%)	0 (0)	1 (6)	0.300
Targeted temperature management, n (%)	23 (64)	16 (100)	0.709
Outcomes			
ICU-Length of Stay, n	6±8	10±26	0.120
Hospital length of stay,	16±23	14±36	0.010
Survival to hospital discharge, n (%)	13 (36)	2 (13)	0.106
Cerebral Performance Category at 6-month follow-up, n (%)			0.106
• 1	13 (36)	2 (13)	
• 2	0 (0)	0 (0)	
• 3	0 (0)	0 (0)	
• 4	0 (0)	0 (0)	
• 5	21 (58)	14 (87)	

M=male; F=female; CPR=cardiopulmonary resuscitation; ECMO=extracorporeal membrane oxygenation; IABP=intra-aortic balloon pump; ICU=intensive care unit.

Table 4. Lung CT-scan quantitative analysis in out-of-hospital cardiac arrest patients.

	Manual CC (n=36)	Mechanical CC (n=16)	p-value
Lung density, HU	-663±97	-541±171	0.002
Lung volume, mL	2534±917	2613±812	0.617
Lung gas volume, mL	1698±733	1405±631	0.172
Lung weight, g	837±306	1208±630	0.006
Not inflated lung tissue, %	1±4	9±15	0.025
Poorly inflated lung tissue, %	10±13	21±15	0.007
Well inflated lung tissue, %	89±15	69±28	0.006

Data expressed as mean±SD.

Table 5. Arterial blood gas analyses and respiratory variables of out-of-hospital cardiac arrest patients.

	Manual CC (n=36)	Mechanical CC (n=16)	p
Arterial blood gas analysis at ICU admission			
pH	7.336±0.11	7.214±0.21	0.025
PaCO ₂ , mmHg	38±8	43±12	0.060
PaO ₂ /FiO ₂	328±132	232±103	0.013
BE, mmol/L	-5.3±5.6	-9.6±7	0.028
Lactate, mmol/L	3.9±4	7.7±6	0.015
Ventilatory setting at ICU admission			
Tidal volume, ml	509±77	527±56	0.197
Peak inspiratory pressure, cmH ₂ O	23±5	26±7	0.214
Respiratory rate	15±3	9±7	<0.001
FiO ₂ , %	48±14	71±20	0.028
PEEP, cmH ₂ O	6.1±1.5	7.5±3.0	<0.001
Arterial blood gas analysis 24h after ICU admission			
pH	7.42±0.06	7.404±0.06	0.403
PaCO ₂ , mmHg	37±6	39±5	0.352
PaO ₂ /FiO ₂	344±95	263±106	0.027
BE, mmol/L	-0.5±3.6	-0.44±3.7	0.825
Lactate, mmol/L	2±1.9	2.6±2.3	0.126
Ventilatory setting 24 h after ICU admission			
Tidal volume, ml	496±102	532±93	0.367
Peak inspiratory pressure, cmH ₂ O	20±7	22±4	0.368
Respiratory rate	14±4	8±4	<0.001
PEEP, cmH ₂ O	7.0±2.0	9±3.2	0.021
FiO ₂ , %	40±16	58±21	<0.001

Data expressed as mean±SD. FiO₂ of the natural lung (equal or lower than the FiO₂ of the membrane lung) was used to calculate the PaO₂/FiO₂ in patients with ECMO in the mechanical CC group.

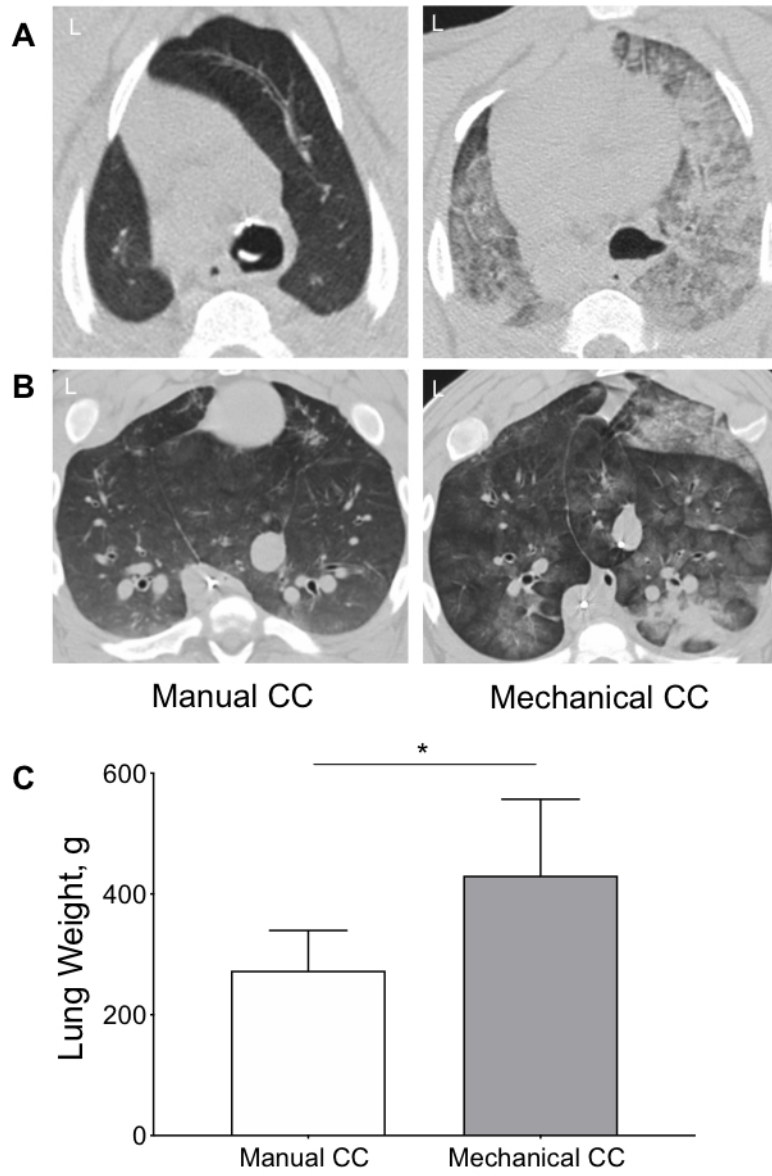
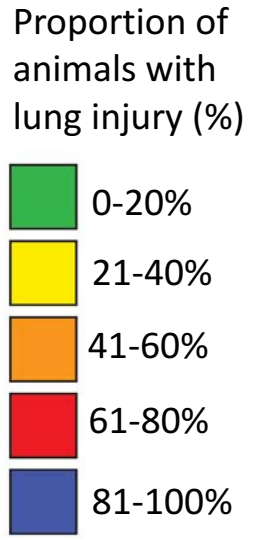
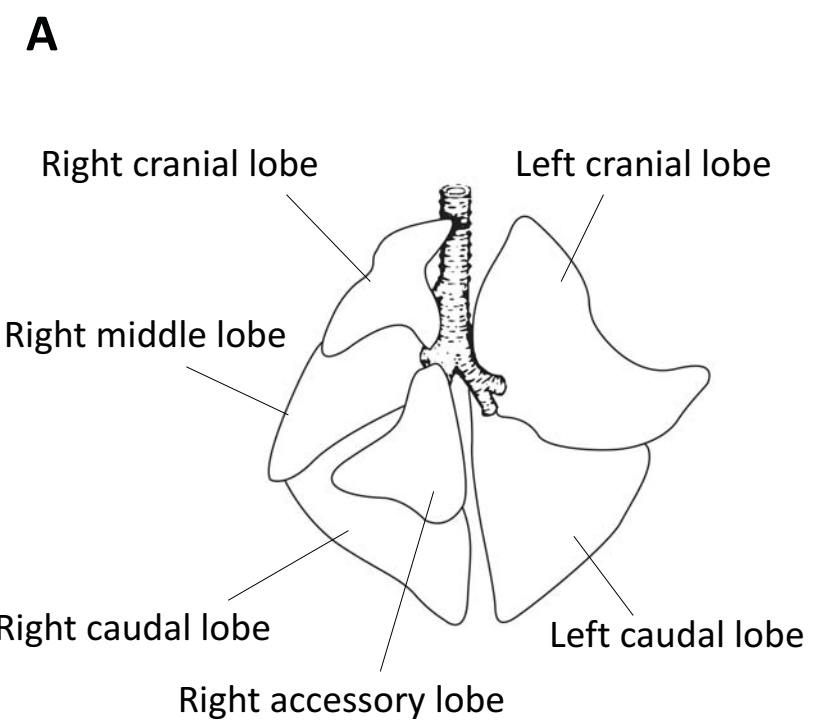


Figure 1

254x330mm (72 x 72 DPI)

Figure 2



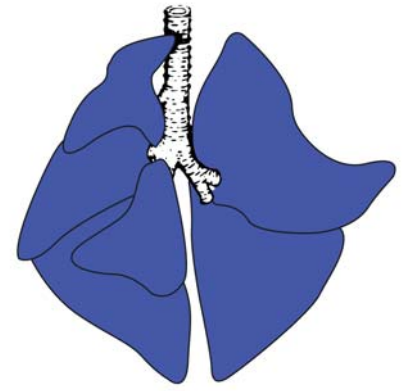
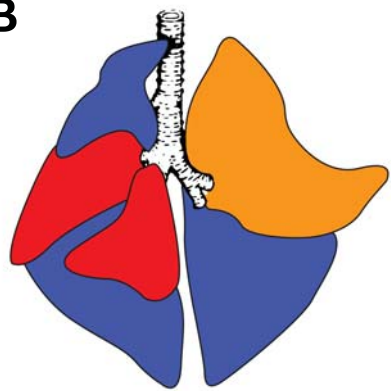
Ground glass attenuation

Manual CC

Mechanical CC

B

C



Airspace Consolidation

D

E

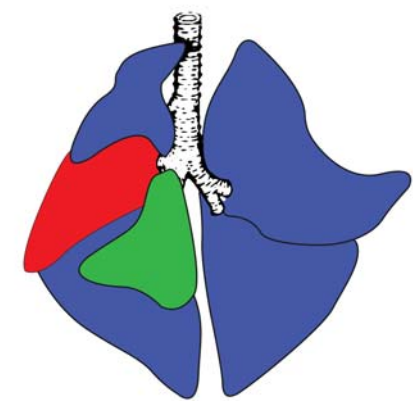
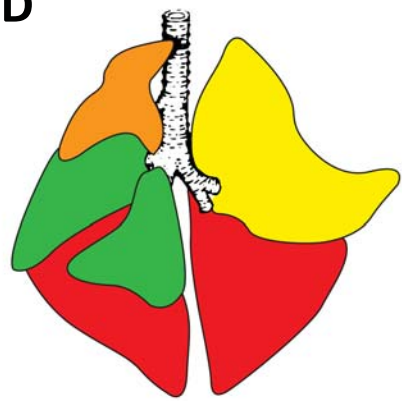


Figure 3

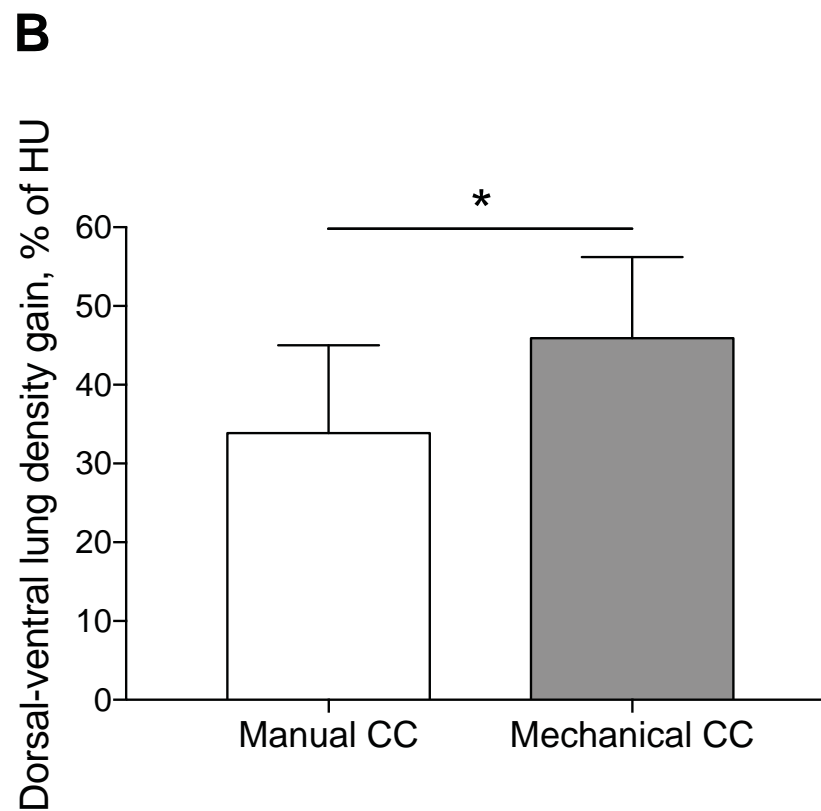
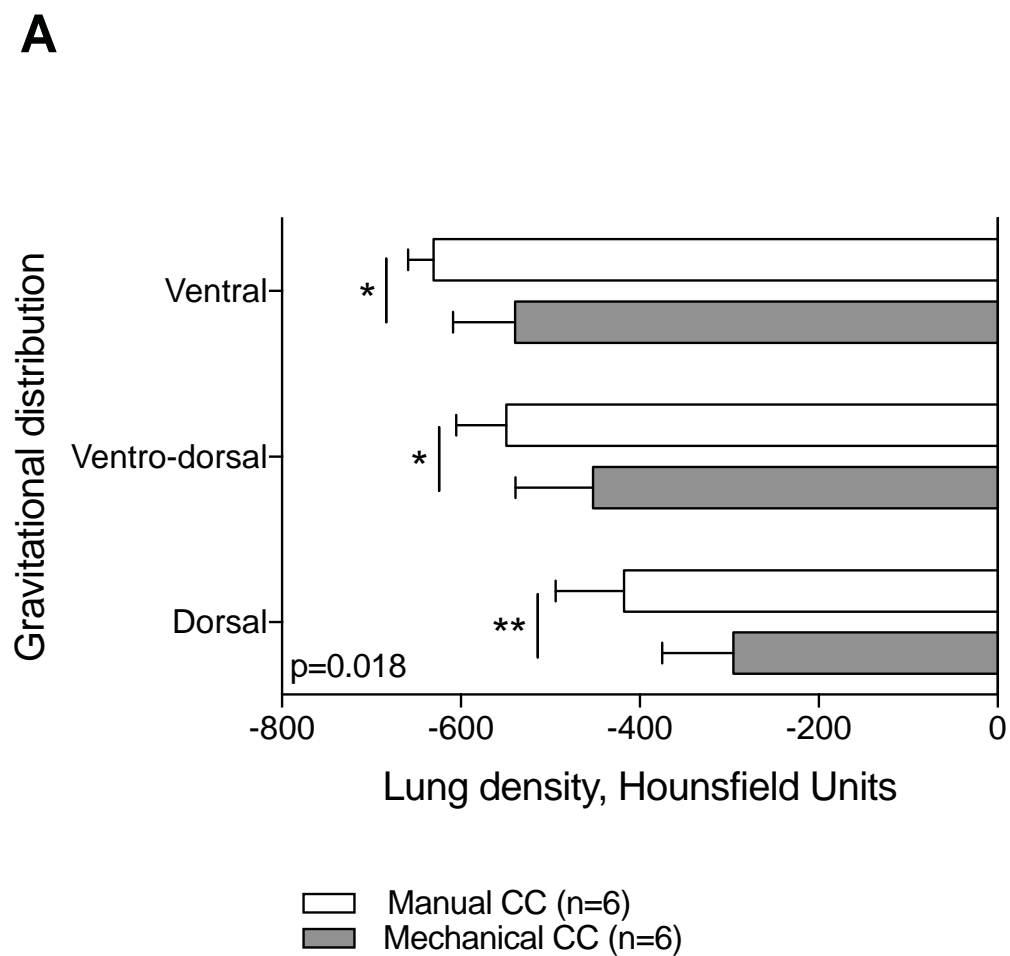


Figure 4

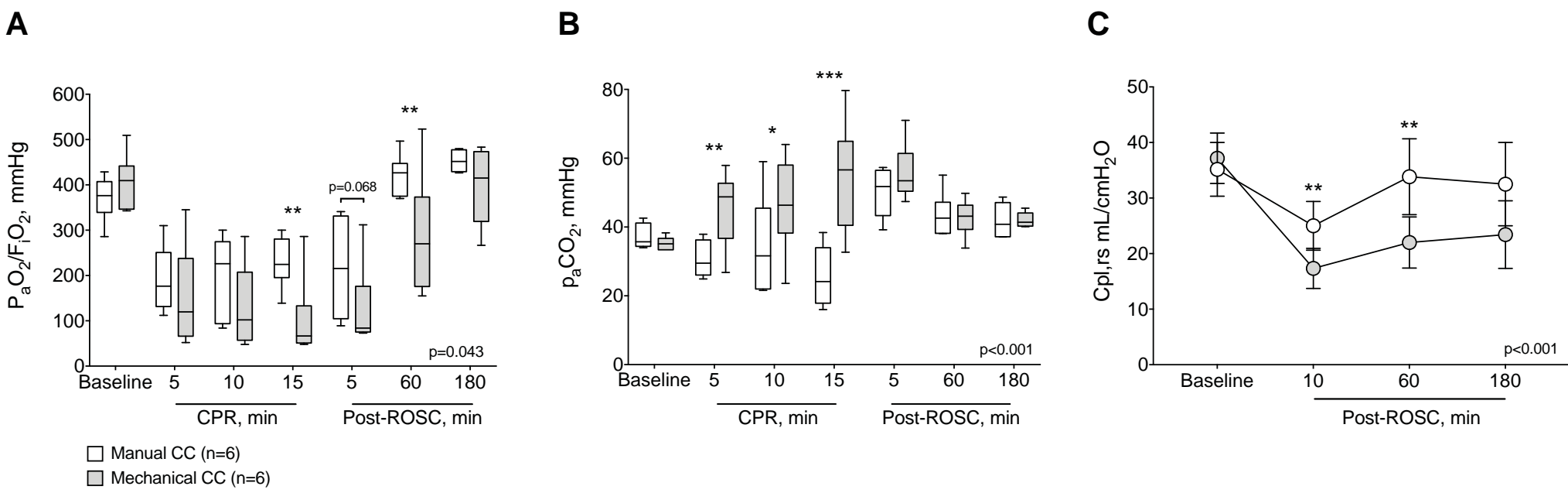


Figure 5

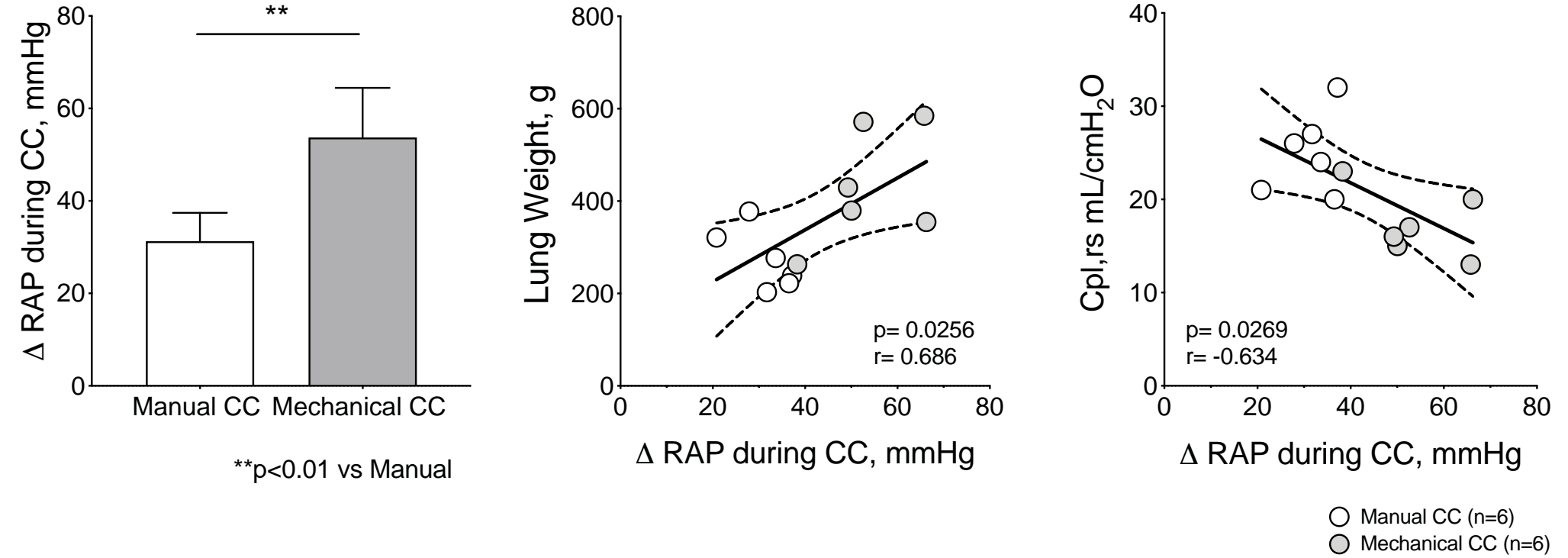
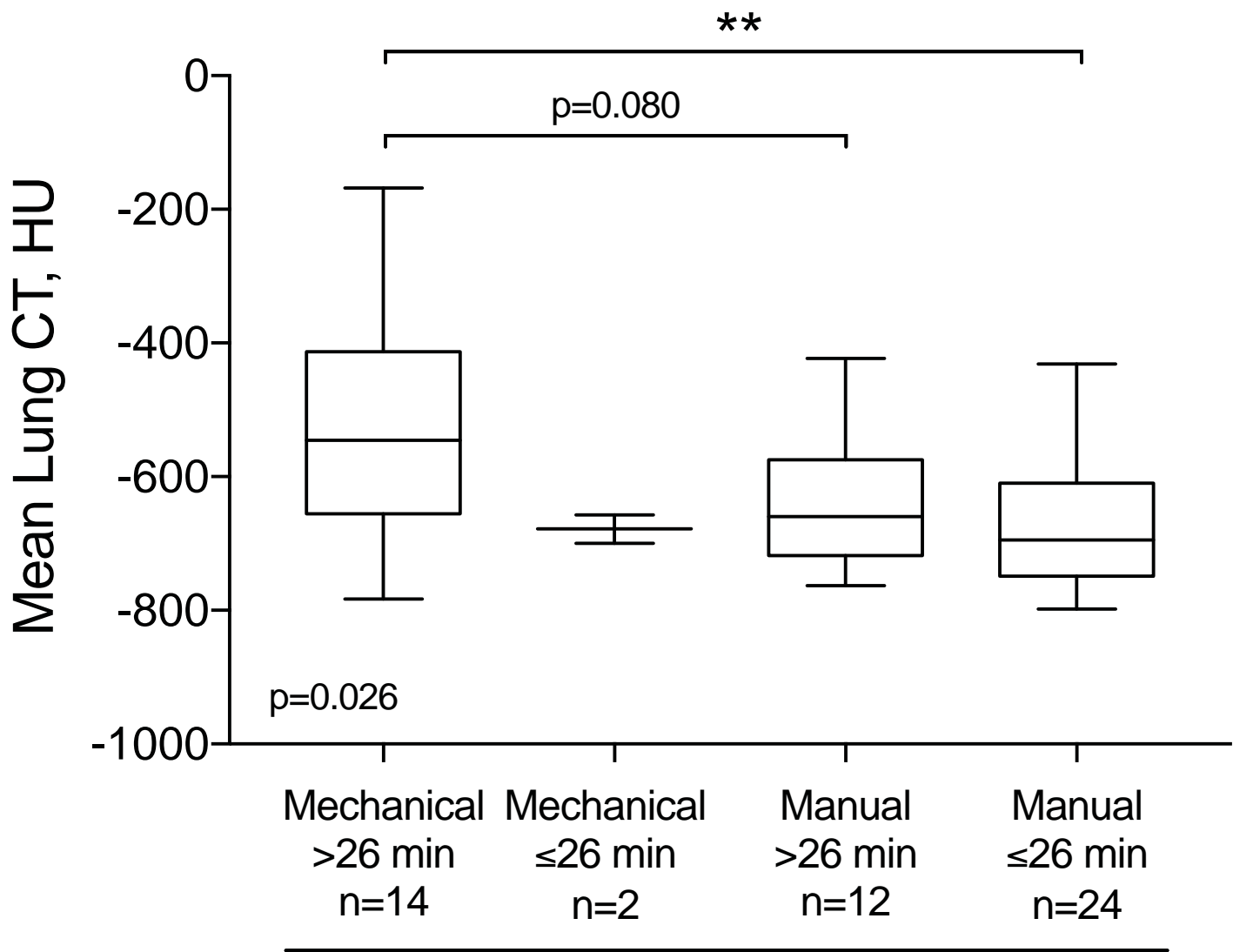


Figure 6



Groups stratified by CC and low-flow time

Online Data Supplement

Cardiopulmonary Resuscitation-Associated Lung Edema (CRALE) - A Translational Study

Aurora Magliocca, Emanuele Rezoagli, Davide Zani, Martina Manfredi, Daria De Giorgio, Davide Olivari, Francesca Fumagalli, Thomas Langer, Leonello Avalli, Giacomo Grasselli, Roberto Latini, Antonio Pesenti, Giacomo Bellani, Giuseppe Ristagno

Methods

This translational study was conducted 1) in a porcine model of CA and prolonged CPR; 2) in a cohort of out-of-hospital CA patients undergoing manual or mechanical CC with a lung CT scan performed after resuscitation.

Experimental study

This is a secondary analysis of a previously published preclinical study (E1) comparing the hemodynamic effect of mechanical versus manual CC during ambulance transportation. We studied twelve successfully resuscitated pigs randomized to mechanical (n=6) or manual (n=6) CC with a thoracic CT scan performed at the end of resuscitation maneuvers.

Ethic statement

Procedures involving animals and their care were conducted in conformity with the institutional guidelines at the Istituto di Ricerche Farmacologiche Mario Negri IRCCS (IRFMN) and Azienda Polo Veterinario di Lodi, Università degli studi di Milano which adheres to the principles set out in the following laws, regulations, and policies governing the care and use of laboratory animals: Italian Governing Law (D.lgs 26/2014; Authorization n.19/2008-A issued March 6, 2008 by Ministry of Health); Mario Negri Institutional Regulations and Policies providing internal authorization for persons conducting animal experiments (Quality Management System Certificate – UNI EN ISO 9001:2008 – Reg. N° 6121); the EU directives and guidelines (EEC Council Directive 2010/63/UE). They were reviewed and approved by the Mario Negri and Università di Milano Institute of Animal Care and Use Committee, which includes ad hoc members for ethical issues, and by the Italian Ministry of Health (Decreto no. 26/2014, authorization no. 979/2017-PR). Animal facilities meet international standards and are regularly checked by a certified veterinarian who is

responsible for health monitoring, animal welfare supervision, experimental protocols and review of procedures.

Animal preparation

Twelve male domestic swine (34.0 ± 1.4 kg) were fasted with free water access the night before the experiments. Anesthesia was induced by intramuscular injection of ketamine (20 mg/kg) followed by intravenous administration of propofol (2 mg/kg) and sufentanyl (0.3 μ g/kg) through an ear vein access. Anesthesia was maintained with a continuous intravenous infusion of propofol (4-8 mg/kg/h) and sufentanyl (0.3 μ g/kg/h). A cuffed endotracheal tube was placed, and animals were mechanically ventilated in volume-controlled mode with a tidal volume of 15 mL/kg, a fraction of inspired oxygen (FiO_2) of 0.21, and a positive-end expiratory pressure of 5 cmH₂O, I:E 1:2 at baseline (Bellavista 1000, IMT Medical, Switzerland). Respiratory rate was adjusted to maintain the end-tidal partial pressure of carbon dioxide (EtCO_2) between 35 and 40 mmHg, using an infrared capnometer (LIFEPAK® 15 monitor/defibrillator, Physio-Control, WA, USA). For measurements of aortic pressure and right atrial pressure fluid-filled 7F catheters were used. Frontal plane electrocardiogram (ECG) was recorded.

Experimental procedure

Animals were randomized by the sealed envelope method to receive mechanical or manual CC, before the induction of cardiac arrest. 1-2 mA alternating current delivered to the endocardium of the right ventricle was used to induce ventricular fibrillation (VF). Mechanical ventilation was discontinued after onset of VF and the endotracheal tube was left open to room air. After 2 min of untreated VF, continuous CC with one of the two strategies (mechanical or manual) was started and performed for 18 min during ambulance transportation. Unsynchronized mechanical ventilation was resumed simultaneously to CC,

with the following parameters: volume-controlled mode with tidal volume of 15 mL/kg, respiratory rate of 10 breaths/min, inspiratory to expiratory ratio (I:E) 1 to 1.5, FiO₂ of 1.0 and zero positive end-expiratory pressure (ZEEP) (Oxylog 1000, Dräger, Lübeck, Germany). Every 5 min during CPR, epinephrine (1 mg) was administered via the right atrium, while arterial blood samples were obtained. Manual CC was provided in accordance to 2015 international CPR guidelines (E2). Mechanical CC was delivered by the LUCAS® 3.0 chest compression system (Stryker/Jolife AB, Lund, Physio-Control, Sweden), which delivers continuous CC (rate: 102±2 per min; depth: 53±2 mm; duty cycle: 50±5%). In the first 3 min of CPR the ambulance was stationary, for the following 15 min the ambulance moved along a predefined itinerary inside the veterinary campus.

After the 18-min interval of CPR, defibrillation was attempted with a single biphasic 200-Joule shock, using a LIFEPAK® 15 monitor/defibrillator. Return of spontaneous circulation (ROSC) was defined as the presence of sinus rhythm with a mean arterial pressure (MAP) of more than 60 mmHg. If ROSC was not achieved, CPR was resumed and continued for 1 min prior to a subsequent defibrillation with an escalating energy strategy (300-360-J). If VF reoccurred after ROSC, an immediate defibrillation was delivered. The same resuscitation protocol was continued until successful resuscitation or for a maximum of 5 additional min. 10 min after ROSC a lung computed tomography (CT) was performed and then animals were monitored for additional 3 h, under anesthesia. A continuous infusion of propofol (4-8 mg/kg/h) and sufentanyl (0.3 µg/kg/h) was provided through an ear vein access. Post ROSC mechanical ventilation was provided using volume-controlled mode with the following parameters: tidal volume 15 mL/kg, positive-end expiratory pressure of 5 cmH₂O, I:E 1:2, a fraction of inspired oxygen (FiO₂) of 0.21-0.4 (Bellavista 1000, IMT Medical, Switzerland).

Measurements

ECG, hemodynamics (arterial and right atrial pressures), EtCO₂, and esophageal temperature were continuously recorded with two LIFEPAK® 15 monitor/defibrillators. All data were then stored on CODE-STAT 9.0 (Physio-Control, WA, USA) and exported as comma separated values (.csv) to LabChart 8.0 (ADInstruments, UK) for the analysis. For each minute of CPR the minimum, the maximum and the swing in right atrial pressure were computed. The variation of right atrial pressure (Δ RAP) was reported as surrogate of intrathoracic pressure (ITP). Compliance of the respiratory system (Cpl_{rs}) was assessed at baseline and up to 3h after ROSC using dynamic compliance calculated using recursive least square algorithm, with a sample rate of 200Hz by the ventilator (Bellavista 1000, IMT Medical, Switzerland). Arterial blood gas analyses were assessed with i-STAT System (Abbott Laboratories, Princeton, NJ).

When blood was withdrawn from the animals, it was immediately centrifuged, and plasma was aliquoted (200 μ l) and stored at -70°C for biomarker assays. Hs-cTnT was measured with an electrochemiluminescence assay (Cobas, Roche Diagnostics, Rotkreuz, CH). NT-proANP was assayed with a validated ELISA kit (Biomedica BI-20892, Wien, Austria) following the manufacturer's recommendations. Porcine Receptor for advanced glycation end products (RAGE) and Porcine Pulmonary Surfactant Associated Protein D (SPD) were measured with quantitative competitive immunoassay (ABclonal, Cliniscience, Rome, Italy).

Autopsy

At the end of the 72-hour post resuscitation observation, animals were anesthetized for echocardiographic examination and blood sample withdrawn. Animals were then euthanized

painlessly with an intravenous injection of 150 mg/kg sodium thiopental. Lung tissue samples were excised from the ventral portion of the caudal left lobe, with careful dissection from surrounding tissues. Lung tissues were fixed by immersion in 10% formalin for at least 24 h then embedded in paraffin. Five- μ m thick sections were obtained and stained with hematoxylin-eosin. The extent of histologic lung damage (i.e. lung tissue versus alveolar airspace) was determined using quantitative stereological techniques as previously reported (E3).

CT scanning

At the end of the resuscitation maneuvers, a chest computerized tomography (CT) was performed with a 16-slices helical CT scanner (GE Brightspeed Elite®, GE Healthcare, Italy) using the following parameters: 1.25 slice thickness, tube current 220 mA, tube voltage 120 kV, scan speed 1 s/rotation, 0.938:1 pitch, 18.75 mm/rot. The images were reconstructed with a window setting for the evaluation of the lung parenchyma (level -700 HU; width: 1500 HU) and bone tissue (level: 600 HU; width: 3000 HU).

Lung CT scans were performed during breath holding at end-expiration at 5 cmH₂O, with subjects in dorsal recumbency and no contrast media was used. The OsiriX 10.0 software (Pixmeo, Switzerland) was used to perform the morphological analysis of the lung parenchyma.

Lung CT morphological analysis

Two veterinary radiologists, blind to study group assessed lung CT scans in order to describe the presence of the following lung findings: ground-glass attenuation, airspace consolidation, peribronchovascular thickening, interlobular septal thickening, air-bronchogram, and pleural effusion. Ground-glass attenuation and airspace consolidation were defined as an increased

attenuation respectively without or with obscuration of the underlying vasculature. An air-bronchogram was defined as an air-filled bronchus, which could be visualized in the parenchymal opacity (E4). Ground-glass attenuation and airspace consolidation were described in a scale from 0 to 2 as 0=absent, 1=local, 2=diffuse. Rib and sternal fractures were described.

Clinical study

This was a multicenter observational, retrospective cohort study conducted according to the Declaration of Helsinki and followed the Italian guidelines of good clinical practice and Data Protection Code. We recorded patient personal information anonymously using an alphanumeric code and we filed patient data electronically.

We collected the clinical records of out-of-hospital CA patients admitted from 2011-01-01 to 2019-12-01 in the Intensive Care Units (ICU) of three different Italian hospitals (University Hospital San Gerardo, Monza; University Hospital IRCCS Ospedale Maggiore Policlinico, Milano; and University Hospital ASST Grande Ospedale Metropolitano Niguarda, Milano). The promoting center of the study was University Hospital San Gerardo in Monza.

The Ethical Committee Monza-Brianza Province, ASST Monza–Ospedale San Gerardo–Anestesia e Rianimazione, Monza, Italy (promoting center, Ethical Committee Monza N° 3070) and the Ethical Committee of the two collaborating centers (University Hospital IRCCS Ospedale Maggiore Policlinico, Milano Ethical Committee N° 935_2019, and University Hospital ASST Grande Ospedale Metropolitano Niguarda, Milano Ethical Committee N° 181-15042020) approved this study. Informed consent was waived based on the retrospective observational nature of the investigation and as per approval of internal Ethical Committee.

The inclusion criteria were adult patients with out-of-hospital CA of non-traumatic origin who received CPR with either manual or mechanical CCs and underwent a lung CT scan within 24h from the cardiac arrest. Exclusion criteria were presence of aspiration pneumonia, pulmonary thromboembolism, lung cancer, chronic pulmonary diseases and lung CT scan performed after 24 hours of CA.

The following clinical data were retrieved from patient electronic medical records: sex, age, weight, CA characteristics, physiological data including hemodynamics, gas exchanges and ventilator setting, ICU and hospital length-of-stay, hospital mortality.

Patients CT scanning

We analyzed lung CT scan performed at three different institutions. Each CT had been requested by the treating physicians as part of the diagnostic work-up of the patient.

Two helical multislice CT-scanners were used: Philips Tomoscan SR 7000 (Philips Medical Systems, Hamburg, Germany: 120 kV tube voltage, 165 mA/s tube current) and Somatom Definition Flash (Siemens, Munich, Germany: 120 kV voltage 110 mA/second tube current).

Different reconstruction methods were used during routine clinical imaging. Contiguous images were reconstructed with both 2 and 3 mm slice thickness. In patients who received contrast material, only baseline CT scan images without contrast were analysed. Mechanically ventilated patients were scanned during uninterrupted ventilation, as per current clinical practice.

Lung CT quantitative analysis

Quantitative analysis of lung CT scans of experimental CAs and out-of-hospital CA patients

were performed using manual segmentation in blind and published methods for volume and weight measurements (E5-E10).

The manual segmentation of lung parenchyma was performed with manual delineation of each lung (from the internal rib border and the external border of the mediastinum) using the mediastinal window (CT min = -250 HU, CT max = +150 HU). The full CT – scale window (CT min = -1000 HU, CT max = +1000 HU) was used instead to view bronchi, bronchioles, blood vessels, and pleural effusion allowing a more accurate identification of these structures, in order to exclude main vessels/bronchi from the segmentation (E9). Pleural effusion was also excluded from the segmentation.

Ten slices were selected: the most cranial and caudal CT-sections and eight evenly spaced CT-sections between them were analyzed. Each of these ten CT-sections was analyzed using the standard segmentation described above. Previously described densitometry method was used to assess four differently aerated lung compartments in the 10 sections (E5-E8). The results were extrapolated to the entire lung, according to the method described by Reske et al. (E10).

In each slice the lungs were divided into three sterno-vertebral areas of equal height (i.e. ventral, ventro-dorsal and dorsal) in which we computed the number of voxels within each attenuation range: hyper-aerated (-1000 to -901 Hounsfield units [HU]), normally-aerated (-900 to -501 HU), poorly-aerated (-500 to -101 HU) and non-aerated lung parenchyma (-100 to +100 HU). Overall lung density was calculated as the average density of all lung slices normalized by the areas of the lung slices. The gradient of lung density was calculated as $(\text{Ventral HU} - \text{Dorsal HU}) / (\text{ventral HU}) * 100$. Increased lung density was defined in the presence of a mean lung density ≥ -500 HU, as this threshold is known to discriminate the presence of loss versus presence of aeration (E11-E12).

Statistical analysis

Continuous and categorical data were expressed as mean±standard deviation and frequency (percentage), respectively. Normality of distribution of continuous variables was assessed using D'Agostino-Pearson omnibus normality test. Difference among groups for continuous data was assessed using unpaired Student's t-test or Mann-Whitney U test, according to data distribution. Differences in categorical data among groups were assessed using the Fisher's exact test. Differences between the study groups (treatment effect) was evaluated using a two-way analysis of variance for repeated measurements over time (group-by-time interaction). In the presence of a significant test result, a post-hoc analysis was performed by controlling the false discovery rate using a two-stage step-up method of Benjamini, Krieger and Yekutieli for multiple comparisons.

In the morphological analysis of the CT scan findings, the presence of ground glass attenuation (GGA) and airspace consolidation (AC) were evaluated in each of the six lung lobes of each animal. In order to adjust the model for the within animal correlation, difference among groups in the proportion of GGA and AC was calculated using an adjusted logistic regression analysis with robust clustering, where GGA and AC were considered as outcome variable, the type of chest compressions as exposure variable, and the pigs were considered as cluster variable. Graphs were represented using mean±standard deviation or whisker plots. Correlations between continuous data were explored using linear regression analysis. The degree of association was reported using the Pearson's correlation coefficient (r) ranging between -1; +1. In the clinical study, univariate logistic regression analysis was used to evaluate the association of different variables between the manual versus mechanical CC group (i.e. age and low-flow time in Table 3) with the presence of increased lung density. Prolonged or shorter low-flow time was defined for value above or below/equal to the

median value (i.e. 26 minutes). As the number of cases of increased lung density was low (n=9), and the 95%CI was quite wide for both the exposure variable (type of CC) and the confounder (low-flow time) we investigate the role of low-flow time as confounder/effect modifier using as outcome variable – in place of the dichotomic variable increased/normal lung density– the mean lung CT expressed as a continuous variable by HU. Accordingly, we explored the association of low-flow time and type of CC in a univariate linear regression model. To investigate the association between all possible combinations of type of low-flow time and type of CC with the mean lung CT and avoid the use of unstable multivariate models in a limited sample size (n=52), we further explored the associations of the 4 groups of patients with outcome in 4 independent linear regression models (i.e. model A-D). As last, to include the interdependency among the 4 groups of patients that could not be taken into account in model A-D – in which the comparison was always between a single group against all 3 other groups of patients - we performed a non-parametric analysis among the 4 groups of patients using the Kruskal-Wallis test. We then performed post-hoc pairwise comparisons among all possible combinations using a Mann-Whitney U test.

Statistical significance was reached when the p-value <0.05 (two-tailed). Statistical analyses were performed using STATA-14/MP (StataCorp LP, College Station, TX, USA), GraphPad Prism 8.3.0 (GraphPad Software, San Diego, CA, USA) and Microsoft Excel for Mac 2017, Version 15.32.

References:

E1. Magliocca A, Olivari D, De Giorgio D, Zani D, Manfredi M, Boccardo A, Cucino A, Sala G, Babini G, Ruggeri L, Novelli D, Skrifvars MB, Hardig BM, Pravettoni D, Staszewsky L, Latini R, Belloli A, Ristagno G. LUCAS Versus Manual Chest Compression During Ambulance Transport: A Hemodynamic Study in a Porcine Model of Cardiac Arrest. *J Am Heart Assoc.* 2019;8(1):e011189.

E2. Perkins GD, Handley AJ, Koster RW, Castrén M, Smyth MA, Olasveengen T, Monsieurs KG, Raffay V, Gräsner JT, Wenzel V, Ristagno G, Soar J. Adult basic life support and automated external defibrillation section Collaborators. European Resuscitation Council Guidelines for Resuscitation 2015: Section 2. Adult basic life support and automated external defibrillation. *Resuscitation.* 2015;95:81-99.

E3. Hopkins N, Cadogan E, Giles S, et al: Chronic airway infection leads to angiogenesis in the pulmonary circulation. *J Appl Physiol* (1985) 2001; 91:919–928

E4. Komiya K, Ishii H, Murakami J, Yamamoto H, Okada F, Satoh K, Takahashi O, Tobino K, Ichikado K, Johkoh T, Kadota J. Comparison of chest computed tomography features in the acute phase of cardiogenic pulmonary edema and acute respiratory distress syndrome on arrival at the emergency department. *J Thorac Imaging.* 2013;28(5):322-8.

E5. Puybasset L, Cluzel P, Gusman P, Grenier P, Preteux F, Rouby JJ Regional distribution of gas and tissue in acute respiratory distress syndrome. I. Consequences for lung morphology. CT Scan ARDS Study Group. *Intensive Care Med.* 2000;26:857–869.

E6. Gattinoni L, Caironi P, Pelosi P, Goodman LR. What has computed tomography taught us about the acute respiratory distress syndrome? *Am J Respir Crit Care Med.* 2001;164:1701–1711.

E7. Rouby JJ, Puybasset L, Nieszkowska A, Lu Q. Acute respiratory distress syndrome: lessons from computed tomography of the whole lung. *Crit Care Med.* 2003;31(Suppl):S285-295.

E8. Borges JB, Okamoto VN, Matos GF, Caramez MP, Arantes PR, Barros F, Souza CE, Victorino JA, Kacmarek RM, Barbas CS, Carvalho CR, Amato MB. Reversibility of lung collapse and hypoxemia in early acute respiratory distress syndrome. *Am J Respir Crit Care Med.* 2006;174:268-278.

E9. Chiumello D, Marino A, Brioni M, Cigada I, Menga F, Colombo A, Crimella F, Algieri I, Cressoni M, Carlesso E, Gattinoni L. Lung Recruitment Assessed by Respiratory Mechanics and Computed Tomography in Patients with Acute Respiratory Distress Syndrome. What Is the Relationship? *Am J Respir Crit Care Med* 2016;193:1254–1263.

E10. Reske AW, Reske AP, Gast HA, Seiwerts M, Beda A, Gottschaldt U, Josten C, Schreiter D, Heller N, Wrigge H, Amato MB. Extrapolation from ten sections can make CT-based quantification of lung aeration more practicable. *Intensive Care Med.* 2010;36(11):1836-44.

E11. Gattinoni L, Pesenti A, Avalli L, Rossi F, Bombino M. Pressure-volume Curve of Total Respiratory System in Acute Respiratory Failure. Computed Tomographic Scan Study *Am Rev Respir Dis.* 1987 Sep;136(3):730-6.

E12. Gattinoni L, Caironi P, Pelosi P, Goodman LR. What Has Computed Tomography Taught Us About the Acute Respiratory Distress Syndrome? *Am J Respir Crit Care Med.* 2001 Nov 1;164(9):1701-11.

E13. Judge EP, Hughes JM, Egan JJ, Maguire M, Molloy EL, O'Dea S. Anatomy and bronchoscopy of the porcine lung. A model for translational respiratory medicine. *Am J Respir Cell Mol Biol.* 2014 Sep;51(3):334-43.

Supplemental tables

Table E1. Lung morphological CT-scan analysis in the experimental study stratified by lung lobe location.

	Mechanical CC (n=6)	Manual CC (n=6)	p-value
Ground glass attenuation			
Left lobe, n (%)			
• Cranial	5/6 (83)	3/6 (50)	0.545
• Caudal	6/6 (100)	6/6 (100)	/
Right lobe, n (%)			
• Cranial	6/6 (100)	5/6 (83)	1.000
• Middle	6/6 (100)	4/6 (67)	0.455
• Accessory	5/6 (83)	4/6 (67)	1.000
• Caudal	6/6 (100)	6/6 (100)	/
Overall cranial lobes, n (%)*	11/12 (92)	8/12 (67)	0.177
• Local	1/12 (8)	4/12 (33)	0.133
• Diffuse	10/12 (83)	4/12 (33)	0.024
Overall lower lobes, n (%)*	23/24 (96)	20/24 (83)	0.149
• Local	3/24 (12.5)	15/24 (63)	<0.001
• Diffuse	20/24 (83)	5/24 (21)	<0.001
All lobes	34/36 (94)	28/36 (78)	0.144
• Local	4/36 (11)	19/36 (53)	<0.001
• Diffuse	30/36 (83)	9/36 (25)	<0.001
Airspace consolidation			
Left lobe, n (%)			
• Cranial	5/6 (83)	2/6 (33)	0.242
• Caudal	6/6 (100)	4/6 (67)	0.455
Right lobe, n (%)			
• Cranial	5/6 (83)	3/6 (50)	0.545
• Middle	4/6 (67)	1/6 (17)	0.242
• Accessory	0/6 (0)	1/6 (17)	1.000
• Caudal	6/6 (100)	4/6 (67)	0.455
Overall cranial lobes, n (%)*	10/12 (83)	5/12 (42)	0.132
• Local	3/12 (25)	2/12 (17)	0.651
• Diffuse	7/12 (58)	3/12 (25)	0.139
Overall lower lobes, n (%)*	16/24 (67)	10/24 (42)	0.029
• Local	8/24 (33)	5/24 (21)	0.383
• Diffuse	8/24 (33)	5/24 (21)	0.346
All lobes	26/36 (72)	15/36 (42)	0.012
• Local	11/36 (30)	7/36 (19)	0.342
• Diffuse	15/36 (42)	8/36 (22)	0.147

*According to swine lung anatomy lower lobes include middle, accessory and caudal lobes (E13). Overall cranial lobes include both cranial lobes of the left and right lung. Overall lower lobes include both lower lobes of the left and right lung.

Differences among groups were tested by the Fisher's exact test.

Differences of ground glass consolidation and airspace consolidation among the groups for overall cranial and lower, and all lobes were adjusted for the within animal correlation by robust clustering. Significant p-values are reported in bold.

Table E2. Hemodynamic and echocardiographic variables in the experimental study.

	Manual CC (n=6)	Mechanical CC (n=6)	p
Systolic arterial pressure, mmHg			
Baseline	117±25	118±10	0.810
Post-ROSC, 10 min	103±9	113±24	
Post-ROSC, 120 min	107±13	104±7	
Post-ROSC, 180 min	117±14	115±10	
Diastolic arterial pressure, mmHg			
Baseline	84±14	80±13	0.889
Post-ROSC, 10 min	72±11	83±22	
Post-ROSC, 120 min	75±7	70±8	
Post-ROSC, 180 min	89±14	84±9	
Mean arterial pressure, mmHg			
Baseline	103±14	97±12	0.961
Post-ROSC, 10 min	82±10	93±22	
Post-ROSC, 120 min	89±9	85±8	
Post-ROSC, 180 min	98±16	97±12	
Right atrial pressure, mmHg			
Baseline	5±3	5±2	0.340
Post-ROSC, 10 min	8±2	9±2	
Post-ROSC, 120 min	5±2	6±3	
Post-ROSC, 180 min	6±3	7±3	
Heart rate, bpm			
Baseline	77±19	77±15	0.165
Post-ROSC, 10 min	124±24	159±50	
Post-ROSC, 120 min	114±24	121±36	
Post-ROSC, 180 min	111±19	110±29	
CO, L/min			
Baseline	2.9±0.4	3.4±0.4	0.408
Post-ROSC, 180 min	2.9±0.5	2.7±0.5	
Post-ROSC, 72 h	3.6±1.4	3.9±0.8	
LVEF, %			
Baseline	71±8	68±8	0.912
Post-ROSC, 180 min	53±24	57±12	
Post-ROSC, 72 h	77±5	77±4	
EDV, mL			
Baseline	27±6	29±5	0.571
Post-ROSC, 180 min	33±9	36±9	
Post-ROSC, 72 h	37±4	39±14	
ESV, mL			
Baseline	7±2	9±3	0.795
Post-ROSC, 180 min	17±11	16±9	
Post-ROSC, 72 h	9±3	9±5	

ROSC=return of spontaneous consciousness; CO=cardiac output; EDV=end diastolic volume; ESV=end systolic volume; LVEF=left ventricle ejection fraction. Data expressed as mean±SD. Two-tailed p-value of treatment in a repeated measurements two-way analysis of variance.

Table E3. Hemodynamic characteristics of out of hospital cardiac arrest patients at ICU admission.

	Manual CC (n=36)	Mechanical CC (n=16)	p
Hemodynamic variables			
Systolic arterial pressure, mmHg	120±15	102±28	0.005
Diastolic arterial pressure, mmHg	73±13	69±13	0.283
Mean arterial pressure, mmHg	89±12	80±14	0.026
Heart rate, bpm	76±19	94±23	0.008
Central venous pressure, mmHg	8±3	11±4	0.023
ScVO ₂ , %	74±9	73±10	0.801
SOFA Cardiovascular	2.0±1.5	3.3±0.8	0.045

ScVO₂=central venous oxygen saturation; SOFA=sequential organ failure assessment score.

Table E4.

A) Univariate analyses of association among the type of chest compressions (CC) and significantly different variables between the 2 groups (mechanical versus manual CC, see Table 3) with increased lung density (number of events=9), defined as a lung mean CT HU within the whole lung ≥ 500 (categorical binomial data).

Variable	OR	95% CI	p
Age	0.97	0.93 – 1.02	0.236
Low flow time >26 minutes (Ref. Low Flow time \leq 26 minutes)	4.42	0.82 – 23.79	0.083
Mechanical CC (Ref. Manual CC)	6.6	1.39 – 31.28	0.017

B) Univariate analysis of association among the type of chest compressions (CC) and significantly different variables between the 2 groups (mechanical versus manual CC, see Table 3) with a higher lung CT density expressed as mean HU within the whole lung (continuous data).

Variable	β Coefficient	95% CI	p
Age	-1.55	-4.00 – 0.91	0.211
Low flow time >26 minutes (Ref. Low Flow time \leq 26 minutes)	96.31	25.25 – 167.36	0.009
Mechanical CC (Ref. Manual CC)	122.18	47.35 – 197.01	0.002

Table E5. Possible combinations of type of low-flow time and type of CC in patients with the mean lung CT of patients with out-of-hospital CA by 4 independent linear regression models.

Variable	β Coefficient	95% CI	p
Mechanical CC by Low flow time >26 minutes (Ref. Other patients) (14 versus 38 patients)	142.68	67.02 – 218.34	<0.001
Mechanical CC with Low flow time \leq 26 minutes (Ref. Other patients) (2 versus 50 patients)	-55.28	-252.63 – 142.06	0.576
Manual CC with Low flow time >26 minutes (Ref. Other patients) (12 versus 40 patients)	-22.50	-112.63 – 67.63	0.618
Manual CC with Low flow time \leq 26 minutes (Ref. Other patients) (24 versus 28 patients)	-88.65	-160.75 – -16.56	0.017

We investigated in 4 independent linear regression models (Model A-D) the association between low-flow time and type of CC with the mean lung CT. Patients undergoing mechanical CC and a prolonged low flow time (Model A) showed a strong positive correlation with mean lung density; in contrast, patients undergoing manual CC and with a shorter low flow time (model D) showed a negative correlation with mean lung density.

Supplemental figures

Figure E1. Correlation between lung weight (A) and lung volume (B) with compliance of the respiratory system (Cpl,rs).

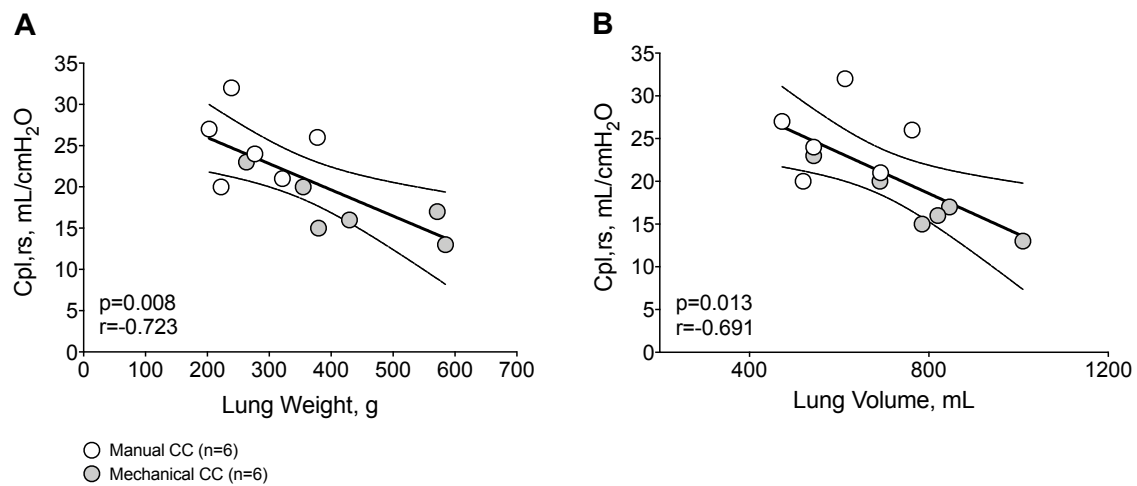


Figure E2. Representative image of in right atrial pressure variation (Δ RAP) during manual and mechanical CC.

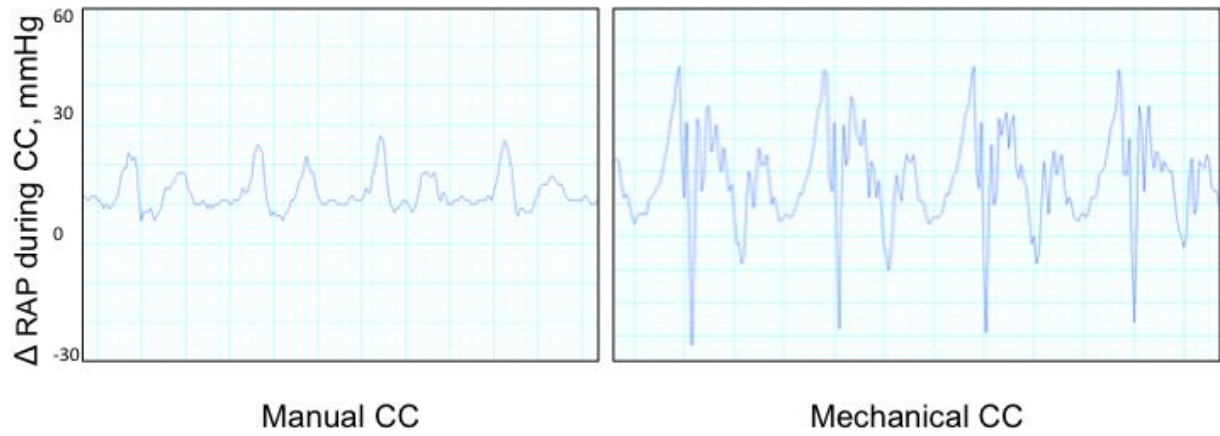


Figure E3. Differences in right atrial pressure variation (Δ RAP) among experimental groups over 18 minutes of cardiopulmonary resuscitation. Two tailed p-value of the difference among groups in a repeated measurements two-way analysis of variance.

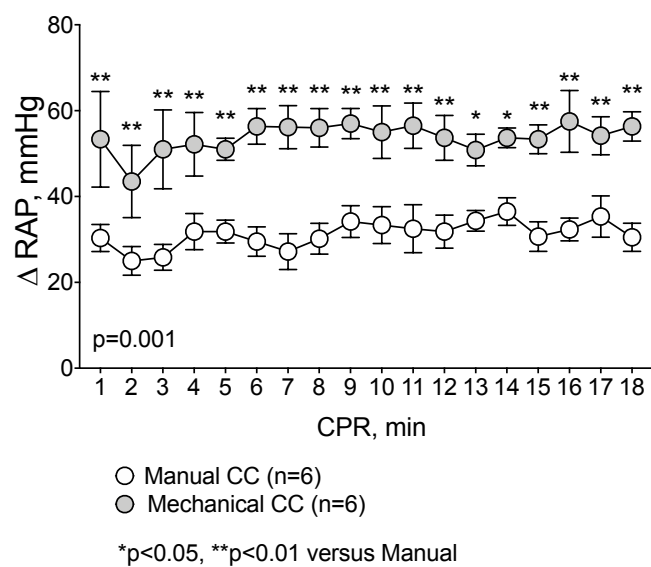


Figure E4. Differences in biomarkers of hemodynamic impairment (NT-proANP and TnT, A and B respectively) and lung injury (RAGE and SPD, C and D respectively) in plasma between experimental groups over 3-day follow-up. Two tailed p-value of the difference among groups in a repeated measurements two-way analysis of variance.

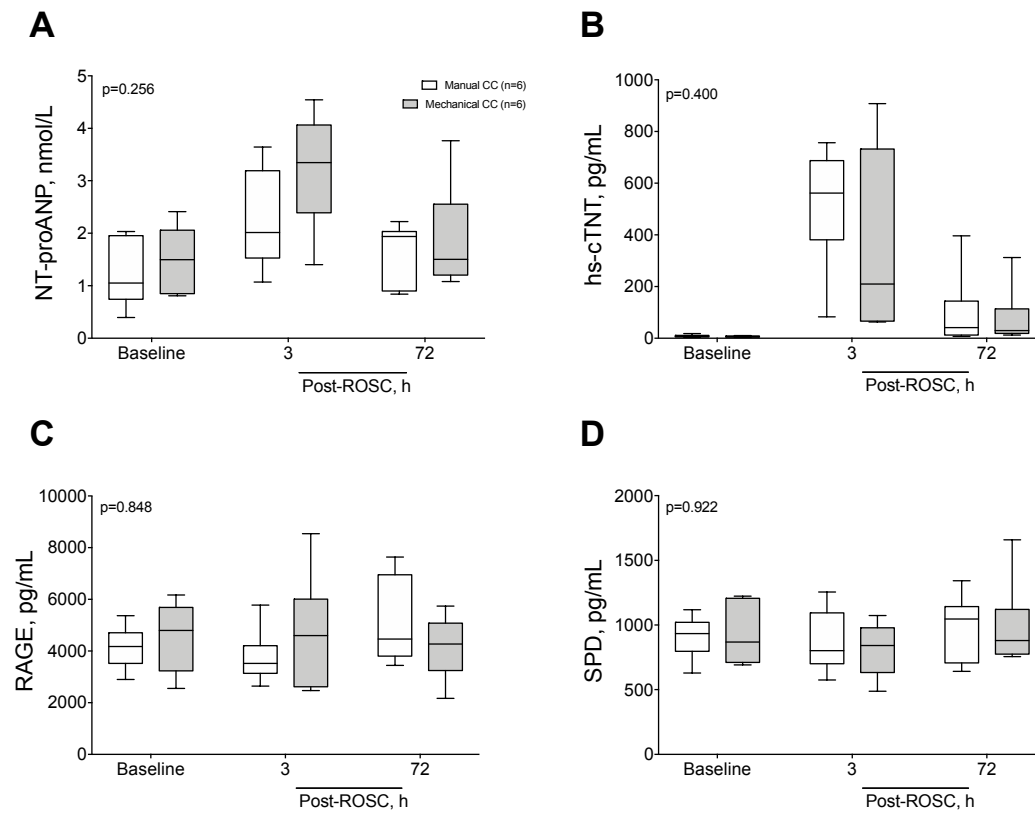


Figure E5. Histology of lung tissue at animal necropsy. Differences of alveolar lung tissue and alveolar airspace among experimental groups. Two tailed p-value of the difference among groups in a repeated measurements two-way analysis of variance.

